

Continuous-Time Nonlinear Model Predictive Control based on Pontryagin Minimum Principle and Penalty Functions

*Original*

Continuous-Time Nonlinear Model Predictive Control based on Pontryagin Minimum Principle and Penalty Functions / Pagone, M., Boggio, M., Novara, C., Proskurnikov, A., Calafiore, G.. - In: INTERNATIONAL JOURNAL OF CONTROL. - ISSN 0020-7179. - STAMPA. - (2025). [10.1080/00207179.2024.2366432]

*Availability:*

This version is available at: 11583/2989549 since: 2024-06-19T09:09:27Z

*Publisher:*

Taylor & Francis

*Published*

DOI:10.1080/00207179.2024.2366432

*Terms of use:*

This article is made available under terms and conditions as specified in the corresponding bibliographic description in the repository

*Publisher copyright*

Taylor and Francis postprint/Author's Accepted Manuscript

This is an Accepted Manuscript of an article published by Taylor & Francis in INTERNATIONAL JOURNAL OF CONTROL on 2025, available at <http://www.tandfonline.com/10.1080/00207179.2024.2366432>

(Article begins on next page)

ARTICLE TEMPLATE

## Continuous-Time Nonlinear Model Predictive Control based on Pontryagin Minimum Principle and Penalty Functions

Michele Pagone <sup>a</sup>, Mattia Boggio <sup>a</sup>, Carlo Novara <sup>a</sup>, Anton Proskurnikov <sup>a</sup>, and Giuseppe Carlo Calafiore<sup>a</sup>

<sup>a</sup>Department of Electronics and Telecommunications, Politecnico di Torino, Corso Duca degli Abruzzi, 24, 10129 Turin, Italy

### ARTICLE HISTORY

Compiled June 14, 2024

### ABSTRACT

Pontryagin's Minimum Principle (PMP) is a powerful tool for solving Nonlinear Model Predictive Control problems (NMPC), enabling the handling of time-varying input constraints and cost functions. However, applying PMP encounters challenges when state constraints must be satisfied. This arises because the optimal trajectory often requires a blend of unconstrained and constrained arcs with unknown junction points. To address this issue, relaxation methods are frequently explored, where state constraints are replaced with penalty functions.

The contributions of this paper are as follows. First, a method of penalty functions allowing for coping with soft state constraints is examined. We prove the recursive feasibility of this method and demonstrate its efficiency in a numerical example. Second, the finite-time practical stability for the optimal reference tracking NMPC problem is addressed. By appropriately choosing the terminal cost, one can guarantee the convergence of the state vector to a predefined neighborhood of the target state.

### KEYWORDS

Nonlinear control systems; predictive control; stability; constrained control.

## 1. Introduction

Model Predictive Control has garnered significant attention from both academic and industrial researchers, emerging as a reliable control tool across a wide range of applications (Rawlings et al., 2022). MPC offers optimal control algorithms for multi-dimensional systems that operate under state, input, and output constraints. Recent advancements in electronics and optimization have enabled the real-time implementation of MPC on embedded processors (Deng & Ohtsuka, 2022).

A crucial aspect of MPC design involves devising solvers for receding horizon optimal control problems (OCP). Among these, convex optimization solvers stand out as the most efficient solution. Linear and quadratic programming techniques (Boggio et al.,

---

CONTACT Michele Pagone. Email: michele.pagone@polito.it

CONTACT Mattia Boggio. Email: mattia.boggio@polito.it

CONTACT Carlo Novara. Email: carlo.novara@polito.it

CONTACT Anton Proskurnikov. Email: anton.p.1982@ieee.org

CONTACT Giuseppe Carlo Calafiore. Email: giuseppe.calafiore@polito.it

2022; Dubljevic & Humaloja, 2020; Guerrero-Fernandez et al., 2023; Okawa & Nonaka, 2021; Vidano et al., 2022) are widely applied in MPC problems characterized by linear plant dynamics and constraints, and either linear or convex quadratic performance indices. For systems with nonlinear dynamics, Nonlinear Model Predictive Control (NMPC) methods have been developed, see, e.g., Diehl et al. (2007); Gros et al. (2020) and references therein. Dealing with non-convex OCPs, these approaches encounter challenges such as multiple locally optimal solutions and the absence of algorithms capable of finding the global optimum in polynomial time.

### *Direct vs. Indirect NMPC algorithms*

The dynamics of physical plants, including vehicles, mobile robots, and chemical or biochemical processes, are commonly described by continuous-time equations. Consequently, the OCP to be solved at each iteration of the NMPC procedure becomes a non-convex optimization problem in an infinite-dimensional space. As discussed in (Diehl et al., 2007), NMPC methods can be classified as *direct* or *indirect* depending on how this OCP is handled. Direct NMPC methods reduce the OCP to mathematical programming in a finite-dimensional space by discretizing continuous-time state and input signals and replacing the integral functional with a finite sum. In contrast, indirect methods exploit infinite-dimensional necessary conditions of optimality such as Pontryagin’s minimum principle or the Hamilton-Jacobi-Bellman equations.

An important advantage of direct methods is the availability of various algorithms for online numerical optimization, including Newton’s method and its accelerated modifications. However, these methods suffer from the curse of dimensionality, as the number of variables grows exponentially with the system’s dimension. Additionally, they may fail to find the global extremum in cases of non-convex OCPs. Moreover, because the physical system’s variables are replaced by vectors of parameters, the relationship between the optimal control and state vectors becomes intricate (Allgöwer et al., 2004; Cisneros & Werner, 2020), making real-time control computation troublesome.

To enhance computational efficiency and address these restrictions, explicit NMPC methods have been proposed (Grancharova & Johansen, 2012). These methods involve an offline procedure of partitioning the state space into regions where the controller can be explicitly determined. Typically, the nonlinear OCP is approximated using multi-parametric quadratic programming, enabling the controller to be expressed as a piecewise-affine function of the state (Tondel et al., 2003a); fast procedures for determining the region containing a given state vector facilitate efficient implementation of this controller (Tondel et al., 2003b). If the nonlinear dynamics of the plant are unknown or too complex, a data-driven explicit NMPC approach can be used. This approach replaces the genuine plant with its data-based approximation, such as a neural ARX network (Grancharova & Johansen, 2012, Ch. 8), fuzzy models (Alcalá et al., 2022; Boumaza & Belarbi, 2022; Mendes et al., 2022), or a model resulting from set-membership identification (Boggio et al., 2023).

It should be noted that indirect methods can cope with *exact* continuous-time models, whereas direct methods (including the explicit NMPC methods) deal with sampled time (or even data-driven) approximations of the actual dynamics. Indirect NMPC algorithms, avoiding sampling of the state and input signals, are more accurate, as will be demonstrated numerically in Section 4. At the same time, their performance is comparable to direct methods thanks to the efficient solvers of boundary value problems.

## *Pontryagin’s principle, State Constraints and Penalty Methods*

In this paper, we develop an *indirect* approach to NMPC that leverages Pontryagin’s Minimum Principle (PMP), thereby reducing the OCP to a two-point boundary value problem (TPBVP) (Bryson & Ho, 1975; Kvitko, 2020). The PMP-based solvers strike a balance between computational complexity and system performance, being well-suited for real-time applications. Although TPBVPs typically lack analytical solutions, efficient out-of-the-box solvers are available for handling them (Kierzenka & Shampine, 2001; Shampine & al., 2003). Numerical methods employed to solve TPBVPs include shooting (Ha, 2001), stabilized continuation (Ohtsuka & Fujii, 1997; Ohtsuka, 2003), Newton-type algorithms (Deng & Ohtsuka, 2019), modal series and discretization-based methods (Cannon et al., 2008; Devia et al., 2018; Dontchev et al., 2020).

An essential benefit of PMP-based optimization is its capacity to accommodate initial and terminal state constraints. However, its application to optimization problems with geometric (anytime) state constraints is more challenging (Diehl et al., 2007). In this scenario, the optimal trajectory is divided into segments, known as “arcs”, with equations varying depending on whether the state constraints are active (constrained arcs) or inactive (unconstrained arcs). The quantity of constrained and unconstrained arcs in an optimal solution is not predetermined. Furthermore, the necessity for maintaining a smooth state function imposes additional tangency conditions at the junction points (Bonnard et al., 2003; Pesch, 1994). As highlighted by Malisani et al. (2016), in the presence of constrained arcs, PMP gives rise to a complex system of coupled differential-algebraic equations, the solving of which in real-time can be challenging.

To mitigate computational complexity, state (and potentially input) constraints are frequently alleviated by incorporating a *penalty function* into the performance index. Based on the design of this function, relaxation approaches fall into two categories: *interior* and *exterior* penalty methods (Malisani et al., 2016). In both sorts of methods, the weighting of the penalty promotes constraint satisfaction but introduces bias in the optimal solution, leading to deviations from the solution of the original problem.

Interior (barrier) penalty functions prioritize constraint satisfaction over optimality, ensuring strict adherence to the constraint set (Kovaltchouk et al., 2015; Malisani et al., 2016; Suwartadi et al., 2010) by growing infinitely as the solution approaches the boundary of this set. However, unbounded cost functions may introduce numerical challenges and render the optimization ill-posed, making them difficult to use in real-time NMPC. Many frameworks employing barrier functions and constraint relaxation rely on restrictive assumptions, such as a well-defined relative degree for each constraint (Graichen & Petit, 2009; Graichen et al., 2010; Malisani et al., 2016).

Exterior penalty functions penalize violations of constraints considered *soft*, indicating that solutions violating them are physically possible yet highly undesirable. As the penalty weight increases, violations become sufficiently small, prompting the algorithm to prioritize satisfying soft constraints whenever possible. A similar concept is employed in “approximate barrier” functions (Hauser & Saccon, 2006). Exterior barrier functions are common in applications prioritizing input (actuator) constraints over state constraints. Input constraints, such as an actuator’s maximum effort, current/voltage range, or rotation rate, are considered *hard* as violating them is physically impossible. In contrast, state constraints can be violated by physically admissible solutions in unavoidable scenarios (e.g., collisions in autonomous vehicle control). Predicting whether actuators can comply with state constraints is challenging, making safety assurance during optimization difficult. When state constraints conflict with input constraints, barrier methods render optimization infeasible, while exterior penalty

functions ensure the numerical feasibility of OCPs.

### *Contributions and structure of the manuscript*

The contributions of this paper are as follows:

- We examine a Nonlinear Model Predictive Control (NMPC) algorithm based on Pontryagin’s Minimum Principle (PMP), which employs an exterior penalty function to relax state constraints while ensuring compliance with input constraints via PMP equations. This algorithm draws inspiration from Ohtsuka & Fujii (1997); however, that paper addresses a different OCP. Specifically, in Ohtsuka & Fujii (1997), the penalty term is contingent solely upon the terminal state of the system, penalizing entry into forbidden regions solely at the end of the prediction horizon. In contrast, we incorporate the penalty into the integrand, aiming to prevent the system from entering undesired sets at every time instant. This leads to a modification of the boundary value problem resulting from PMP. We demonstrate the efficiency of our algorithm compared to direct NMPC methods, using the predator-prey population dynamics as a case study.
- Whereas Ohtsuka & Fujii (1997) employs a cubic penalty (an unbounded function) instead a Gaussian-like one, without proving recursive feasibility of the algorithm, we formally prove the recursive feasibility of the proposed NMPC algorithm with relaxed state constraints and show that the solution of the closed-loop system always exists and is forward complete.
- Our third contribution involves the stability analysis of the PMP-based NMPC algorithm, where the cost function corresponds to tracking a slow reference signal. Unlike prevailing results on MPC stability in the literature, the plant dynamics are continuous-time, and the problem lacks hard terminal constraints, instead featuring only a terminal cost that penalizes deviation from the desired equilibrium. We demonstrate that with a sufficiently large weight, the terminal cost ensures a weak stability property: all solutions starting in a known bounded neighborhood of the equilibrium are uniformly bounded. Additionally, by tuning the terminal weight, one can induce these solutions to converge within an arbitrarily small pre-designed ball centered at the equilibrium and remain there. This approach guarantees finite-time practical stability.

The rest of this paper is organized as follows. After introducing some notation symbols, in Section 2 the general NMPC framework is introduced. Section 3 applies the PMP to solve the receding horizon optimal control problems, illustrated by numerical simulations in Section 4. In Section 5, we examine local stability of the closed-loop system (the proof of the result is detached into a technical Appendix for the ease of reading). Finally, the conclusions are drawn in Section 6.

### *Notation*

Henceforth the symbol  $\doteq$  should be read as “defined by”. The symbols  $\mathbb{R}$  and  $\mathbb{N}$  denote, respectively, the sets of all real and all natural numbers.

Elements of  $\mathbb{R}^n$ , unless otherwise stated, are considered as column vectors of height  $n \in \mathbb{N}$ . The symbol  $\mathbb{R}^{m \times n}$  denotes the set of  $m \times n$  real matrices. The symbol  $\|z\| \doteq \sqrt{z^\top z}$  denotes the standard Euclidean norm of vector  $z \in \mathbb{R}^n$ . More generally, for a positive definite matrix  $\mathbf{W} = \mathbf{W}^\top$ , we introduce the weighted norm  $\|z\|_{\mathbf{W}} \doteq \sqrt{z^\top \mathbf{W} z}$ .

For two matrices  $\mathbf{P} = \mathbf{P}^\top$  and  $\mathbf{Q} = \mathbf{Q}^\top$  of equal dimension, we write  $\mathbf{P} \geq \mathbf{Q}$  if  $\mathbf{P} - \mathbf{Q}$  is positive semidefinite, that is,  $x^\top \mathbf{P} x \geq x^\top \mathbf{Q} x$  for each vector  $x$ .

The symbol  $\nabla$  denotes the gradient operator. Note that for a function  $\varphi : \mathbb{R}^n \rightarrow \mathbb{R}$ ,

the gradient is a *column* of height  $n$ . If function depends on several variables, e.g.,  $\varphi = \varphi(x, z)$ , we write  $\nabla_x \varphi$  to denote the gradient with respect to  $x$ .

## 2. The general continuous-time NMPC Framework

Consider a nonlinear affine system governed by the following equation

$$\dot{x}(t) = f(x(t)) + g(x(t))u(t), \quad t \geq 0, \quad (1)$$

where  $x(t) \in \mathbb{R}^{n_x}$ ,  $u(t) \in \mathbb{R}^{n_u}$  are, respectively, the state and the input vectors at time  $t$ . Throughout the paper, we assume that this equation is uniquely solvable for each bounded input signal  $u(\cdot)$ . The state vector and command input are restricted, respectively, by sets  $X_C$  and  $U_C$  in the sense that  $x(t) \in X_C \subseteq \mathbb{R}^{n_x}$ ,  $u(t) \in U_C \subseteq \mathbb{R}^{n_u}$ .

The structure of NMPC algorithm is shown in Fig. 1.

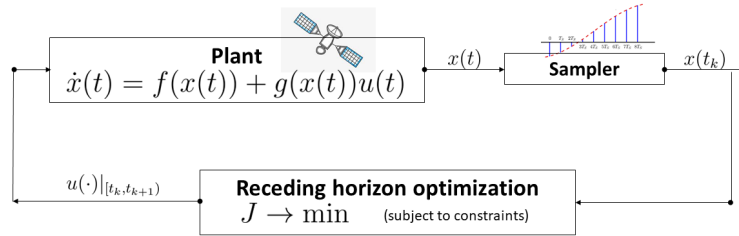


**Figure 1.** The general structure of NMPC algorithm

The measurements of the state vector are sampled with period  $T_S > 0$ . At the  $k$ th sampling instant  $t_k \doteq kT_S$  (where  $k = 0, 1, \dots$ ), the measurement  $x_k \doteq x(t_k)$  is available. Based on this measurement, we compute the control for  $t \in [t_k, t_{k+1})$  by solving the following Bolza-type optimal control problem (OCP)

$$\mathbf{minimize} \quad J = \phi(\hat{x}(t_k + T_p)) + \int_{t_k}^{t_k + T_p} \Phi(\hat{x}(\tau), \hat{u}(\tau)) \, d\tau \quad (2)$$

over the set of all functions  $(\hat{x}, \hat{u})$  that are defined on the predictive time domain<sup>1</sup>  $[t_k, t_k + T_p]$  and satisfy the **constraints**:

$$\begin{aligned} \dot{\hat{x}}(\tau) &= f(\hat{x}(\tau)) + g(\hat{x}(\tau))\hat{u}(\tau), \quad \hat{x}(t_k) = x(t_k) \\ \hat{x}(\tau) &\in X_C \subset \mathbb{R}^{n_x}, \quad \hat{u}(\tau) \in U_C \subset \mathbb{R}^{n_u}, \quad \forall \tau \in [t_k, t_k + T_p], \end{aligned} \quad (3)$$

Here  $T_p = nT_S$  (where  $n \geq 1$  is integer) is the *prediction horizon*. Functions  $\phi: \mathbb{R}^{n_x} \rightarrow \mathbb{R}$ ,  $\Phi: \mathbb{R}^{n_x + n_u} \rightarrow \mathbb{R}$  are called the *terminal* and *integral costs* respectively.

Upon finding the optimal solution  $(\hat{x}_k^*, \hat{u}_k^*)$  in (3), the actual control on the interval  $[t_k, t_{k+1})$  is defined as

$$u(t) = \hat{u}_k^*(t) \quad \forall t \in [t_k, t_{k+1}), \quad (4)$$

<sup>1</sup>Henceforth, all signals defined on the *predictive* time interval are denoted by symbols with  $\hat{\cdot}$ , e.g.,  $\hat{x}, \hat{u}$  etc., in order to distinguish them from the functions defined on the actual time axis.

whereas the “tail” of optimal control signal  $u^*(t), t > t_{k+1}$  is *not* used for control. At time  $t = t_{k+1}$  the optimization procedure is solved again with the updated measurement  $x(t_{k+1})$ . Hence, the state trajectory  $x(t)$  is also coincident with  $\hat{x}_k^*(t)$  only on  $[t_k, t_{k+1})$ . As usual, the MPC design results in a mixed feedback-feedforward controller. On one hand, the control is *feedforward* (open-loop) between the sampling instants, on the other hand, each control signal  $\hat{u}_k^*$  is based on the measurement  $x(t_k)$ .

As discussed in the introduction, NMPC algorithms can be categorized as either direct or indirect, depending on how the OCP represented by equations (2) and (3) is approached. Direct methods (commonly known as ‘first discretize, then optimize’) approximate this OCP with a finite-dimensional mathematical programming problem. In this work, we focus on *indirect* methods (‘first optimize, then discretize’), which solve the original OCP through Pontryagin’s Minimum Principle.

### 3. Problem Setup. The PMP-based NMPC solver

We first introduce our key assumptions on the system’s dynamics, constraint sets and performance index.

#### *Key assumptions and notation*

Since we are going to apply Pontryagin’s optimality principle to the receding horizon OCP (2), (3), we assume that the system’s dynamics is smooth with respect to the state variable (Bryson & Ho, 1975). Notice that the following assumption also guarantees that the solution to (1) on each sampling interval  $[t_k, t_{k+1})$  is uniquely determined by the input (4) and the state  $x(t_k)$ .

**Assumption 3.1.** *Let  $f \in \mathcal{C}^1(\mathbb{R}^{n_x} \rightarrow \mathbb{R}^{n_x})$  and  $g \in \mathcal{C}^1(\mathbb{R}^{n_x} \rightarrow \mathbb{R}^{n_x \times n_u})$ .*

We confine ourselves to the following typical constraint sets.

**Assumption 3.2.** *The set of admissible inputs is a hyper-rectangle  $U_C \doteq \{u \in \mathbb{R}^{n_u} : u_{i_{min}} \leq u_i \leq u_{i_{max}}\}$ .*

**Assumption 3.3.** *The state constraint set  $X_C \doteq \{x \in \mathbb{R}^{n_x} : C(x) \leq 0\}$  is a sublevel set of some  $C^1$ -smooth function  $C : \mathbb{R}^{n_x} \rightarrow \mathbb{R}$  (generally, non-convex).*

In the problems we are interested in, the performance index penalizes the deviation of the state from the desired reference value<sup>2</sup>  $x_r$ , on one hand, and the deviation of the command input from the desired reference input  $u_r$ , on the other hand. Hence, the terminal cost is defined as

$$\phi(x) = \|x - x_r\|_{\mathbf{P}}^2, \quad x \in \mathbb{R}^{n_x} \quad (5)$$

whereas the integrand  $\Phi$  is:

$$\Phi(x, u) = \|x - x_r\|_{\mathbf{Q}}^2 + \|u - u_r\|_{\mathbf{R}}^2, \quad x \in \mathbb{R}^{n_x}, u \in \mathbb{R}^{n_u}. \quad (6)$$

Here  $\mathbf{P}, \mathbf{Q}, \mathbf{R}$  are positive diagonal matrices of the corresponding dimensions. As a

---

<sup>2</sup>For simplicity, here we assume that the reference is constant. In practice, the controller can be also applied to slowly changing reference signals.

result, we obtain the following cost functional

$$J(\hat{x}, \hat{u}) = \int_{t_k}^{t_k+T_p} (\|\hat{x}(\tau) - x_r\|_{\mathbf{Q}}^2 + \|\hat{u}(\tau) - u_r\|_{\mathbf{R}}^2) d\tau + \|\hat{x}(t_k + T_p) - x_r\|_{\mathbf{P}}^2. \quad (7)$$

Notice that, although the functional is convex, the optimization problem, obviously, is non-convex due to nonlinear dynamics (1) and non-convex state constraint in (3).

**Remark 1.** In (7), we present the most general formulation in which  $J$  accounts for an input reference signal  $u_r$ . A more common NMPC setting (as it will be shown in Section 4) consists in setting  $u_r = 0$ , in order to minimize the control “energy”. On the other hand,  $u_r \neq 0$  can be used for solving problems of pure tracking. Nevertheless, a drawback in setting  $u_r \neq 0$  is that it only works well in nominal conditions, as the input reference depends on  $f(x(t))$  and  $g(x(t))$ .

Pontryagin’s minimum principle (Bryson & Ho, 1975) involves the *Hamiltonian*, which is a function of three independent variables  $x, \lambda \in \mathbb{R}^{n_x}$  and  $u \in \mathbb{R}^{n_u}$ :

$$H(x, u, \lambda) = \Phi(x, u) + \lambda^\top [f(x) + g(x)u] \in \mathbb{R}. \quad (8)$$

### 3.1. Necessary optimality conditions in the case of unconstrained state

Consider first the situation where state constraints are absent:  $X_C = \mathbb{R}^{n_x}$ .

For brevity, we denote the rightmost point of the prediction interval by  $t_k^f \doteq t_k + T_p$ . The necessary conditions of optimality in the OCP (2), (3) are as follows (Bryson & Ho, 1975, Section 2.5). If  $(\hat{x}^*, \hat{u}^*)$  is an optimal solution to the OCP, then function  $\lambda^* : [t_k, t_k^f] \rightarrow \mathbb{R}^{n_x}$  satisfying the following equations

$$\dot{\lambda}^*(t) = -\nabla_x H(\hat{x}^*(t), \hat{u}^*(t), \lambda^*(t)), \quad (9)$$

$$\lambda^*(t_k^f) = \nabla \phi(\hat{x}^*(t_k^f)), \quad (10)$$

$$H(\hat{x}^*(t), \hat{u}^*(t), \lambda^*(t)) = \min_{u \in U_C} H(\hat{x}^*(t), u, \lambda^*(t)) \quad (11)$$

$$\forall t \in [t_k, t_k^f], \quad t_k^f \doteq t_k + T_p. \quad (12)$$

Function  $\lambda^*(\cdot)$  is often referred to as the *co-state* (or *covector*) of an optimal solution.

Adding constraints (3) to the latter equations, one obtains a *two-point boundary value problem* (TPBVP) with  $2n_x$  scalar differential equations for the vector-function  $(\hat{x}^*(t), \lambda^*(t)) \in \mathbb{R}^{2n_x}$ ,  $n_x$  scalar boundary conditions at the leftmost endpoint of the prediction interval, and  $n_x$  boundary conditions at its rightmost endpoint:

$$\begin{aligned} \dot{\hat{x}}^*(t) &= f(\hat{x}^*(t)) + g(\hat{x}^*(t))\hat{u}^*(t), & \hat{x}^*(t_k) &= x_k \\ \dot{\lambda}^*(t) &= -\nabla_x H(\hat{x}^*(t), \hat{u}^*(t), \lambda^*(t)), & \lambda^*(t_k^f) &= \nabla \phi(\hat{x}^*(t_k^f)) \end{aligned}$$

Assuming that this TPBVP is solvable, we can find the desired optimal control from (11). Whereas this procedure can be difficult for a general structure of the Hamiltonian, for our standard cost functions  $\hat{u}^*(t)$  can be found as a function of  $\hat{x}^*(t), \lambda^*(t)$ . The corresponding results are considered in the following subsections.

### Unconstrained Optimization with a Quadratic Cost

The simplest situation is where the constraints on the input are discarded completely  $U_C = \mathbb{R}^{n_u}$ . The Hamiltonian (8) in this situation is

$$H(x, u, \lambda) = (x - x_r)^\top \mathbf{Q}(x - x_r) + (u - u_r)^\top \mathbf{R}(u - u_r) + \lambda^\top (f(x) + g(x)u). \quad (13)$$

The necessary optimality conditions thus become

$$\dot{\lambda}^*(t) = - \left( \frac{\partial f}{\partial x}(\hat{x}^*(t)) + \frac{\partial g}{\partial x}(\hat{x}^*(t))\hat{u}^*(t) \right)^\top \lambda^*(t) - 2\mathbf{Q}(\hat{x}^* - x_r), \quad (14)$$

$$\lambda^*(t_k^f) = 2\mathbf{P} \left( \hat{x}^*(t_k^f) - x_r \right), \quad (15)$$

$$\hat{u}^*(t) = -\frac{1}{2}\mathbf{R}^{-1} \left( g(\hat{x}^*(t))^\top \lambda^*(t) + 2\mathbf{R}u_r(t) \right), \quad (16)$$

$$t \in [t_k, t_k^f]. \quad (17)$$

### Input-Constrained Optimization with a Quadratic Cost

In the situation where the constraint  $\hat{u}(t) \in U_C$  is imposed, where  $U_C$  defined in Assumption 3.2, the necessary optimality conditions are similar, however, the equation for optimal control (16) is replaced by

$$\hat{u}^*(t) = \text{sat}_{U_C} \left[ -\frac{1}{2}\mathbf{R}^{-1} \left( g(\hat{x}^*(t))^\top \lambda^*(t) + 2\mathbf{R}u_r(t) \right) \right] \quad \forall t \in [t_k, t_k^f] \quad (18)$$

where the  $\text{sat}(\cdot)$  is the elementwise saturation operator whose coordinate functions are defined as follows:

$$(\text{sat}_{U_C}(u))_i = \begin{cases} u_{i_{\min}}, & u_i \leq u_{i_{\min}} \\ u_{i_{\max}}, & u_i \geq u_{i_{\max}} \\ u_i, & \text{otherwise.} \end{cases}$$

To prove this, it suffices to notice that  $H$ , considered as a function of a variable  $u_i$ , can be written as

$$H(x, u, \lambda) = r_i u_i^2 - 2r_i u_i u_{r_i} + u_i (g_{\cdot i}(x)^\top \lambda) + \dots = r_i \left( u_i - 2u_i u_{r_i} + \frac{1}{2r_i} (g_{\cdot i}(x)^\top \lambda) \right)^2 + \dots$$

Here the ellipsis stands for the terms independent of  $u_i$ ,  $r_i > 0$  is the  $i$ th diagonal entry of  $\mathbf{R}$ , and  $g_{\cdot i}(x) \in \mathbb{R}_x^n$  is the  $i$ th column of matrix  $g(x)$ . Minimizing the latter function over all  $u_i \in U_C = [u_{i_{\min}}, u_{i_{\max}}]$  and substituting  $\hat{x}^*$ ,  $\hat{u}^*$ ,  $\lambda^*$  into the Hamiltonian, one checks that (11) boils down to (18). Summarizing, we obtain the following lemma (Pagone et al., 2022).

**Lemma 3.4.** *If  $\hat{x}^*$ ,  $\hat{u}^*$  is an optimal solution to (2),(3) with  $J$  defined in (7),  $X_C = \mathbb{R}^{n_x}$  and  $U_C = \{u \in \mathbb{R}^{n_u} : u_{i_{\min}} \leq u_i \leq u_{i_{\max}}\}$ , then a co-state function  $\lambda^*(t)$  exists that satisfies equations (14), (15), and the optimal control obeys (18).*

### 3.2. Relaxation of the (soft) state constraint

In presence of any-time state constraint  $C(x(t)) \leq 0$ , the structure of boundary-value problems depends on the structure of constrained and unconstrained arcs (Bryson & Ho, 1975) (segments of the trajectory where the state constraint is active or inactive, respectively). The arcs and junction points are usually not *a priori* known and can only be found iteratively, which makes algorithms for PMP equation solving difficult for implementation in real time. As shown by Graichen & Petit (2009) and Graichen et al. (2010), state and state-input inequality constraints can be replaced by equalities by augmenting the input vectors and replacing the system of differential equations by differential-algebraic equations. This method, however, imposes a number of restrictions on the constraints, for instance, the relative degree of a constraint must be well defined. To guarantee the absence of singularities, additional regularizing terms are added to the cost function, so the solution returned by the indirect method is only suboptimal (yet converges to the optimal one as the regularizing parameter vanishes).

An alternative approach, which also yields in a suboptimal solution, is to replace the state constraints by additional *penalty terms* in the cost function that are small inside the constraint set  $X_C$  and grow as the state vector approaches its boundary (Wang et al., 2014; Wang & Li, 2017). Assuming that such a function  $\varkappa : \mathbb{R}^{n_x} \rightarrow \mathbb{R}$  is defined, one standard approach (Wang & Li, 2017) is to replace the integrand  $\Phi$  in (2) by

$$\tilde{\Phi}(\hat{x}, \hat{u}) = \Phi(\hat{x}, \hat{u}) + \varkappa(\hat{x}),$$

which corresponds to the augmented performance index

$$\tilde{J}(\hat{x}(\cdot), \hat{u}(\cdot)) = J(\hat{x}(\cdot), \hat{u}(\cdot)) + \int_{t_k}^{t_k+T_P} \varkappa(\hat{x}(\tau)) d\tau. \quad (19)$$

An important advantage of this approach is that the PMP applied to the augmented leads to the standard two-point boundary value problem and does not require to work with constrained and unconstrained arcs of an optimal trajectory. Unlike Ohtsuka & Fujii (1997), the penalty function here is added to the integrand, penalizing thus the constraint violation at *every* time rather than at the end of the prediction horizon.

Often  $\varkappa$  is chosen to be a barrier (or interior penalty) function (Malisani et al., 2016; Wang & Li, 2017) that grows infinite at the boundary of  $X_C$ , preventing thus the optimal trajectory from crossing the boundary. This allows to prove that the state constraints are not violated (provided that the optimization problem is feasible), however, the penalty term in (19) in this case can dominate over the original cost  $J$  destroying thus the optimality. Furthermore, this can lead to numerical instability when solving the boundary-value problems, making the equations ill-posed.

In many applications, state constraints are “soft” in the sense that they may become infeasible in some situations of emergency. An example is the collision avoidance problem in control of mobile robots: one in some situations, it is not possible to evade an obstacle due to limited actuators’ capabilities, even though such a collision leads to substantial damage. Since the NMPC algorithm cannot be stopped in case of infeasible constraints and must return the best possible solution, we need to relax the state constraint. This corresponds to the idea of (exterior) penalty functions  $\varkappa(x)$  that is well-defined and finite on the whole space  $\mathbb{R}^{n_x}$ , reaching its maximum at the boundary of  $X_C$  and rapidly vanishing as the distance from  $x$  to  $\partial X_C$  is growing. This allows to prevent numerical singularities during the solutions, although the solution  $\hat{x}$  can escape

from the predefined set  $X_C$ . As will be discussed in the numerical simulation section, this effect can be mitigated by a proper choice of the penalty function's parameters.

**Assumption 3.5.** *The penalty function is  $\varkappa$  is  $C^1$ -smooth.*

Recalling that  $X_C = \{x \in \mathbb{R}^{n_x} : C(x) \leq 0\}$ , we typically use the Gaussian-like penalty  $\varkappa(x) = a \exp(-bC(x)^2)$  function, where  $a, b$  are parameters to be tuned. Note that the penalty cost  $\varkappa(x)$  reaches the maximum value when  $C(x) = 0$  and then it rapidly decays as  $|C(x)|$  grows; at the same time,  $\varkappa(x)$  can be small when  $C(x) > 0$  (the constraint is violated). The choice of parameters  $a, b$  will be clarified in Section 4 devoted to the numerical example.

### 3.3. The resulting NMPC algorithm and final remarks

In this section, we summarize the procedure for online computation of the control input  $u_k^*$  on each sampling interval  $[t_k, t_k + T_S]$ .

**Preliminaries.** Define three positive diagonal matrices  $\mathbf{P}, \mathbf{Q}$  (of size  $n_x \times n_x$ ) and  $\mathbf{R}$  (of size  $n_u \times n_u$ ) and a penalty function  $\varkappa(x)$  (in the absence of state constraint, let  $\varkappa \equiv 0$ ). Consider the performance index of Bolza type (2) where the terminal cost is quadratic (5) and the integrand has structure as in (7). The augmented performance index  $\tilde{J}$  from (19) is also in the Bolza form (2) with the only difference that the integrand is replaced by  $\tilde{\Phi}(\hat{x}, \hat{u}) = \Phi(\hat{x}, \hat{u}) + \varkappa(\hat{x})$ . The corresponding Hamiltonian is

$$\tilde{H}(\hat{x}, \hat{u}, \lambda) = H(\hat{x}, \hat{u}, \lambda) + \varkappa(\hat{x}).$$

Recall that the original Hamiltonian  $H$  is written either as (13).

**PMP-based NMPC.** To find the control input on each sampling interval  $[t_k, t_{k+1})$ , where  $k = 0, 1, \dots$  solve the following TPBVP on the predictive time domain  $[t_k, t_k + T_p]$

$$\begin{aligned} \dot{\hat{x}}^* &= f(\hat{x}^*) + g(\hat{x}^*)\hat{u}^*, \\ \dot{\lambda}^* &= - \left( \frac{\partial f}{\partial x}(\hat{x}^*(t)) + \frac{\partial g}{\partial x}(\hat{x}^*(t))\hat{u}^*(t) \right)^\top \lambda^*(t) - 2\mathbf{Q}(\hat{x}^* - x_r) - \frac{\partial \varkappa}{\partial x}(\hat{x}^*(t)), \\ \hat{x}^*(t_k) &= x_k, \\ \lambda^*(t_k^f) &= \nabla \phi(\hat{x}^*(t_k^f)) = \lambda^*(t_k^f) = 2\mathbf{P}(\hat{x}^*(t_k^f) - x_r). \end{aligned} \quad (20)$$

To make system (20) closed, one has to substitute the expression for  $\hat{u}^*$  from, respectively, (16) (unconstrained input), and (18) (constrained input).

Upon finding  $\lambda^*(t_k)$  from (20), compute  $\hat{u}^*(t_k)$  as a function of  $\hat{x}^*(t_k) = x_k$  and  $\lambda^*(t_k)$  by using the corresponding equation (16) or (18). Finally, the (actual) control input on the sampling interval  $[t_k, t_{k+1})$  is defined as  $u(t) \equiv u_k = \hat{u}^*(t_k)$ .

The PMP-based NMPC solution is summarized in the Algorithm 1.

**Remark 2.** In practice, the zero-order hold (ZOH) approximation of control signal (4)

$$u(t) \equiv \hat{u}_k^*(t_k) \quad \forall t \in [t_k, t_{k+1}). \quad (21)$$

is often applied. In this situation, the actual state trajectory  $x(t)$  differs from the

---

**Algorithm 1** The iterative procedure of control computation

---

- 1: **Input:**  $t_k, x_k$
  - 2: Define the TPBVP by substituting the relevant equation (16) or (18) into (20).
  - 3: Solve the TPBVP and find  $\hat{x}^*(t_k), \lambda^*(t_k)$ .
  - 4: Determine  $\hat{u}^*(t), t \in [t_k, t_{k+1})$  from the relevant equation (16) or (18).
  - 5: The control input on time interval  $t \in [t_k, t_{k+1})$  is  $u(t) \equiv \hat{u}^*(t)$ .
  - 6: **Output:**  $\hat{u}^*(\cdot)$ .
- 

optimal state trajectory  $\hat{x}_k^*(t)$  even for  $t \in [t_k, t_{k+1})$ , because the *actual* command input (21) differs from (4). Simulations show that the performance of the resulting controller does not deteriorate compared to (4) if the sampling time  $T_S$  is small enough, that is,  $x(t)$  and  $\hat{x}_k^*(t)$  remain close as  $t \in [t_k, t_{k+1})$ . The controller (21), obviously, satisfies the input constraint  $u(t) \in U_C$ .

If the ZOH approximation (21) is used, then the control input computed on Step 5 of Algorithm 1 is replaced by  $u(t) \equiv u(t_k)$ .

## 4. Numerical Example

In this section, we consider an example for validating the presented methodology and compare the PMP-based NMPC solver with direct NMPC methods. In particular, we are going to analyze the case of the constrained Lotka-Volterra model for the population control of a biological system.

### 4.1. The Lotka-Volterra Population Dynamics

Consider the classical predatory-prey Lotka-Volterra model, described by a couple of first-order nonlinear differential equations (Zhang et al., 2016), with an exogenous input applied to both states:

$$\begin{cases} \dot{x}_1 = x_1(\alpha - \beta x_2) + x_1 u_1 \\ \dot{x}_2 = x_2(\gamma x_1 - \delta) + x_2 u_2 \end{cases} \quad (22)$$

where  $x_1$  and  $x_2$  are the prey and predator population respectively and  $u_1$  and  $u_2$  the corresponding input components. Let  $\alpha, \beta, \gamma$ , and  $\delta$  be positive parameters describing the interaction between the two species. The admissible input set is  $U_C \equiv \mathbb{R}^{n_u}$ . Concerning the state constraints, the admissible state set is

$$X_C = \{x(t) \in \mathbb{R}^2 : 5 - \sqrt{(x_1 - 100)^2 + (x_2 - 51.5)^2} \leq 0, \forall t\}, \quad (23)$$

a nonlinear function in charge to prevent the extinction of both species when the predator population grows too abruptly than the prey one. Thus, the state constraints are handled by employing a Gaussian-like function:

$$\varkappa(x) = a \exp(-bC(x)^2) \quad (24)$$

where  $C = 5 - \sqrt{(x_1 - 100)^2 + (x_2 - 51.5)^2}$ ,  $a = 5e5$ , and  $b = 10$ . The penalty function parameters are tuned through a trial and error procedure.

**Table 1.** Dynamics Parameters.

$\alpha$	$\beta$	$\gamma$	$\delta$	$x_0$
0.25	0.25	0.008	0.008	$[40, 40]^T$

**Table 2.** NMPC Parameters.

$T_S$	$T_p$	$\mathbf{R}$	$\mathbf{Q}$	$\mathbf{P}$
0.001 s	0.01 s	$500 \cdot \mathbf{I}_{2 \times 2}$	$diag(10, 35)$	$diag(10, 35)$

In the following example, we employ the quadratic cost function (7) - in the augmented form - including the contribution of the penalty function  $\varkappa(x)$ . Whereby the augmented Hamiltonian:

$$\tilde{H} = \lambda_1(x_1(\alpha - \beta x_2) + x_1 u_1) + \lambda_2(x_2(\gamma x_1 - \delta) + x_2 u_2) + \sum_i^{n_u} r_i u_i^2 + \sum_{i=1}^{n_x} q_i \tilde{x}_i^2 + \varkappa(x). \quad (25)$$

Then, the TPBVP is formalized as:

$$\begin{cases} \dot{x}_1 & = x_1(\alpha - \beta x_2) + x_1 u_1 \\ \dot{x}_2 & = x_2(\gamma x_1 - \delta) + x_2 u_2 \\ \dot{\lambda}_1 & = -\alpha \lambda_2 + \beta \lambda_1 \lambda_2 - \lambda_1 u_1 - \gamma \lambda_2 x_2 - 2\mathbf{Q}_{11} \tilde{x}_1 - \frac{\partial \varkappa(x)}{\partial x_1} \\ \dot{\lambda}_2 & = \beta \lambda_1 x_1 - \gamma \lambda_2 x_1 + \delta \lambda_2 - \lambda_2 u_2 - 2\mathbf{Q}_{22} \tilde{x}_2 - \frac{\partial \varkappa(x)}{\partial x_2} \\ \lambda(t_k + T_p) & = 2\mathbf{P} \tilde{x}(t_k + T_p)^T \end{cases} \quad (26)$$

where  $q_1$  and  $q_2$  are the entries of the diagonal matrix  $\mathbf{Q} \in \mathbb{R}^{2 \times 2}$  and a null reference input is considered. The solution of the TPBVP in (26) provides the values of the state and co-state for the explicit optimal control law:

$$u^* = -\frac{1}{2} \mathbf{R}^{-1} (\lambda^T x) \quad (27)$$

The parameters featuring the Lotka-Volterra dynamics are listed in Table 1 and the NMPC parameters in Table 2, while the following time-varying state reference signal is considered:

$$[x_{r_1}(t), x_{r_2}(t)]^T = [10 \cos(t) + 100, 10 \sin(t) + 50]^T \quad (28)$$

while  $u_r = 0$ . Moreover, as reported in Table 1 the initial state is  $x_0 = [40, 40]^T$ . This means that prey and predator populations are far more than zero, that is the two species are both far from the risk of extinction.

In Figure 2, the phase-plane curve of predator-prey populations is shown. As can be seen, according to the considered configuration, a different trajectory is produced. In particular, we want to highlight how the NMPC approach is perfectly able to avoid the constraint, without affecting the tracking performance. Figure 3 displays the time evolution of populations  $x_1$  and  $x_2$ , and the corresponding tracking errors  $\tilde{x}_1 \doteq x_1 - x_{r_1}$  and  $\tilde{x}_2 \doteq x_2 - x_{r_2}$ . It can be noted that the latter has a very fast

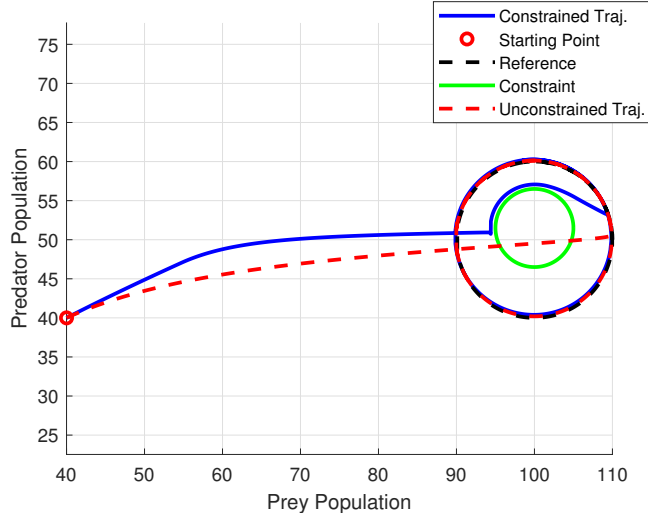


**Figure 2.** Predator-prey populations phase-plane

convergence to zero, proving the effectiveness of the optimization algorithm. Finally, in Figure 4, the command activity is reported.

#### 4.2. Comparison to direct NMPC methods

We are now interested in comparing the behavior of the solutions when employing different optimization strategies.

In detail, we compare the PMP-based NMPC approach with the following direct NMPC methods: i) Sequential Quadratic Programming (SQP), ii) Interior Point (IP), and iii) Nelder-Mead (NM) method (Lagarias et al., 1998). The SQP and IP methods are first-order methods, meaning that they use gradient information to minimize the objective function. Conversely, the NM method is a zero-order method, i.e. it does not require gradient information to optimize the objective function. Instead, it iteratively explores the search domain by moving geometric figures.

For each direct NMPC method, we consider two different cases: i) constant input parametrization, and ii) piece-wise constant input parametrization with  $N = 10$ . In the latter case, the input is parametrized with the same sampling steps used in the PMP-based solution. Indeed, direct optimization methods require the optimal control problem in (2)-(3) to be discretized, in terms of state, input, and constraints (Boiroux & Jørgensen, 2019). Concerning the finite parametrization of the input signal  $u$ , a piece-wise constant parametrization is assumed, with changes of value at the nodes  $\tau_1, \dots, \tau_N \in [t_k, t_k + T_p]$  with  $N$  the number of nodes. Given the number and location of the nodes, the Matlab built-in Matlab solver creates a parameterization with the given  $N$  (Lagarias et al., 1998). To distinguish between the different cases, we will use the following abbreviations: SQP-1, IP-1, NM-1 to indicate constant input, and SQP-10, IP-10, NM-10 to indicate piece-wise constant input with 10 intervals of constancy.

The different optimization strategies were simulated on a Dell Precision 5820 (Processor: Intel® Xeon® W-2123 CPU @ 3.60 GHz). The optimization problem was solved using the following Matlab functions: `bvp5c` for PMP, `fmincon` for SQP and IP, and `fminsearch` for NM. The performance of all algorithms was compared using

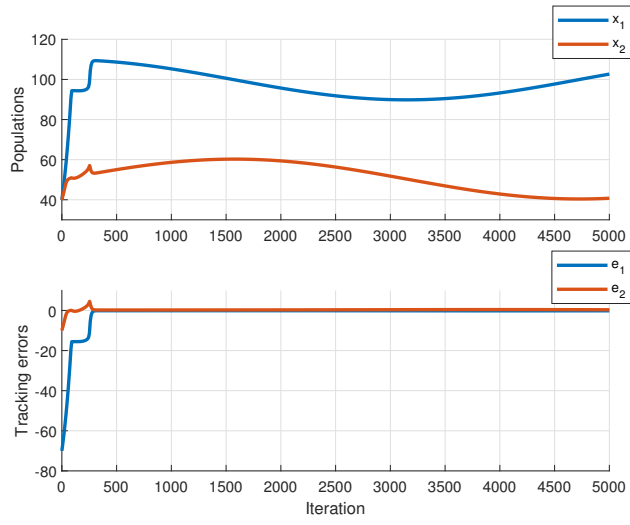


**Figure 3.** Temporal evolution of populations and corresponding tracking errors

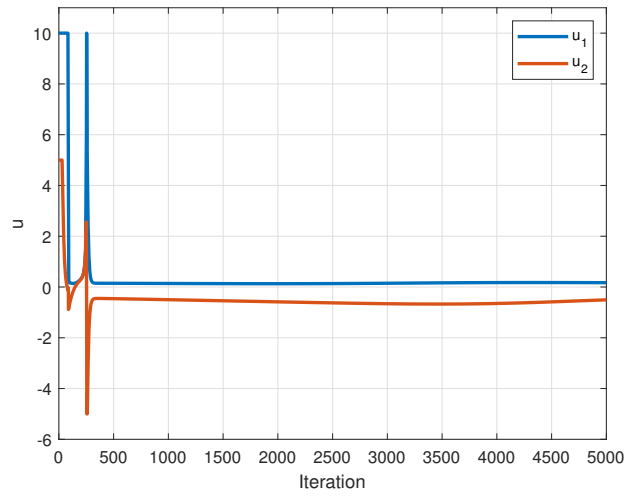


**Figure 4.** Control components

these three metrics:

- (1) Mean Computational Time (Mean C. T.);
- (2) Maximum Computational Time (Max C. T.);
- (3) Standard Deviation of the Computational Time (SD C. T.);
- (4) Mean Reference Tracking Error (Mean Ref. Tr. Er.).

Note that for the computation of the Mean Ref. Tr. Er., the average value of the euclidean distance between the reference and the state of the LV system is considered.

Table 3 presents the performance of the different methods based on the above metrics in the unconstrained case. It can be seen that the PMP-NMPC outperforms the other methods in all the aspects. Indeed, from the mean computational time point of view, the proposed approach is able to obtain results at least four times better than the direct NMPC methods with the same input parameterization (SQP-10, IP-10 and NM-10). Moreover, it exhibits better computational efficiency even when compared to direct NMPC methods with constant input (SQP-1, IP-1 and NM-1). The same considerations hold also for the maximum computational time, the standard deviation and the reference tracking error. Therefore, the proposed PMP-based NMPC framework offers twofold advantages over direct NMPC methods: it achieves a better reference tracking accuracy while requiring less computational time (even compared to the methods that use constant inputs throughout the prediction horizon).

**Table 3.** Comparison between PMP-based and Direct NMPC

	<b>PMP</b>	<b>SQP-1</b>	<b>IP-1</b>	<b>NM-1</b>	<b>SQP-10</b>	<b>IP-10</b>	<b>NM-10</b>
Mean C. T. [ms]	4.5	7.2	6.3	15.6	19.4	21.7	198.6
Max. C. T. [ms]	14.6	28.7	33.3	72	273.8	373.1	464.2
SD C. T. [ms]	0.25	1.4	1.5	1.6	18.8	19.3	52.6
Mean Ref. Tr. Er.	0.173	0.376	0.375	0.376	0.201	0.200	0.214

Figure 5 reports the phase plane for the PMP-NMPC approach and the two SQP methods. In line with the results presented in Table 3, the resulting trajectories confirm the performance advantage of the proposed method.

In Figure 6, a comparison of the computational times for each method is presented. For ease in reading, the results of NM-10 are omitted as their values are at least an order of magnitude larger than the others. As can be seen, the PMP-based NMPC exhibits both the lowest mean value and the smallest standard deviation. This latter advantage is due to its reduced susceptibility to the numerical problems commonly faced with direct methods.

**Remark 3.** By considering the optimal control laws (16) and (18), the values of the input  $u^*$  - along the prediction horizon  $[t_k, t_k + T_p]$  - depend on  $\lambda$  and  $x$ , whose values change at each sampling step of the TPBVP. For this reason, the PMP-based NMPC solution does not require an a-priori parametrization of the input signal. This is a very interesting result since the OCP algorithm achieves high performances without increasing the computational complexity and without any a-priori assumption about the input signal shape. The choice of  $N > 1$  can lead to satisfactory tracking per-

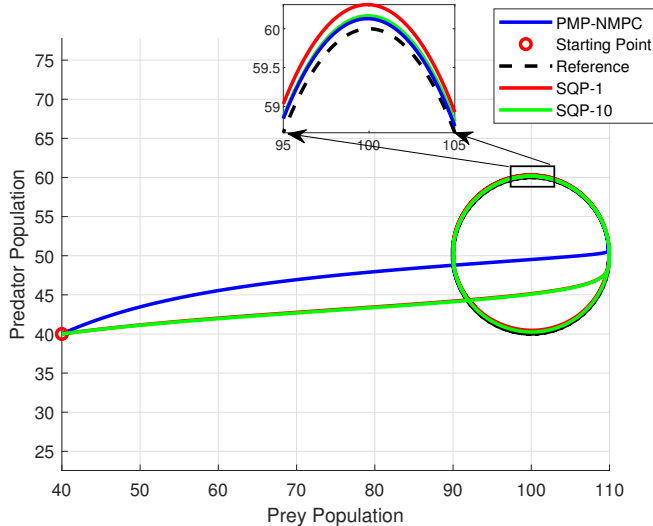


Figure 5. PMP-NMPC, SQP-1 and SQP-10 phase-plane

formances, but at cost of computational complexity increment. On the other hand, choosing  $N = 1$  (i.e., a constant input for every  $\tau \in [t_k, t_k + T_P]$ ) ensures the reduction of the optimization algorithm computational complexity. Nevertheless, this approach could not always guarantee an acceptable level of tracking performance. This issue can be mitigated when employing the PMP-based solution. Indeed, this latter does not require any a-priori assumption about the control signal parametrization and it does not significantly affect the algorithm’s computational complexity.

## 5. Feasibility and Stability of NMPC algorithms

In this section, we examine feasibility and local stability of the NMPC algorithm. This section is structured as follows. We first answer a basic question on whether the NMPC scheme is principle feasible, that is, cannot is happen that the solution of the closed-loop system always exists and is forward complete. In the next subsection, we formulate a simple lemma based on the Gronwall inequality and some standard existence results in optimal control theory. Next, we examine stability a more difficult problem of *stability* of the NMPC scheme in the special situation where the reference point  $(x_r, u_r)$  is an equilibrium of the nonlinear system. It should be noted the most of existing results on the MPC stability focus on equilibrium stabilization.

For the convenience of reading, the proofs of all results of this section are collected in Appendix.

### 5.1. Feasibility of the NMPC scheme

We first prove that the NMPC algorithm is well-posed if the following assumption is adopted; essentially, this assumption is needed to prevent the “blow-up” of a solution of (1) in finite-time for each bounded input  $u(\cdot)$ . Without such an assumption, it is difficult to guarantee the existence of a solution between sampling instants.

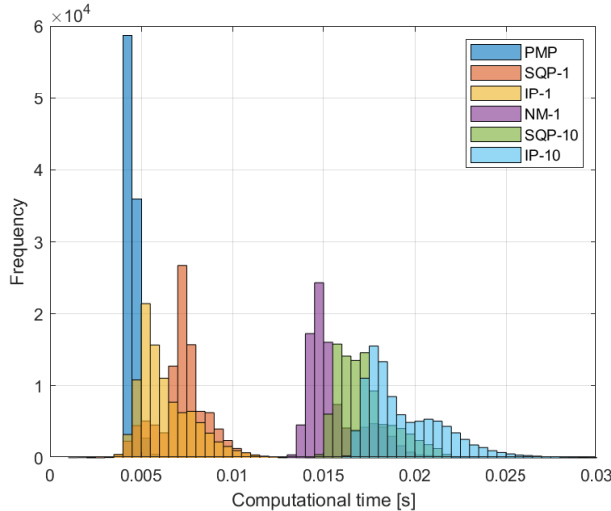


**Figure 6.** Histogram of the computational time

**Assumption 5.1.** For each  $T > 0$  and the initial condition  $x_0$ , there exists  $R = R(x_0, T)$  such that for any solution to (1) with  $x(0) = x_0$  and  $u : [0, T] \rightarrow U_C$  one has

$$\|x(t)\| \leq R \quad \forall t \in [0, T].$$

The structure of our OCP problems, if Assumption 5.1 holds, automatically guarantees the *recursive feasibility* of the arising OCP, being one of the main concerns in analysis of MPC algorithms<sup>3</sup>. We formulate the corresponding lemma.

**Lemma 5.2.** Consider the OCP of minimizing the augmented cost function (19) with constraints (3). Assume that  $f, g, \varkappa$  are  $C^1$ -smooth, the terminal cost is given by (5) and the integral cost is the function in (6). Let  $U_C$  be a compact convex set in  $\mathbb{R}^{u_m}$  (for instance, obey Assumption 3.2). Suppose, finally, that Assumption 5.1 hold. Then, for every  $x(0) \in \mathbb{R}^{n_x}$ , the solution of the closed-loop system is well defined, that is,

- (1) at each  $t_k = kT_s, k = 0, 1, 2, \dots$ , a minimizer  $(\hat{x}_k^*, \hat{u}_k^*)$  exists<sup>4</sup> in the OCP (2),(3);
- (2) the solution to (1) starting at  $x_k = x(t_k)$  and corresponding to the input  $u(t) = \hat{u}_k^*(t)$  exists on the closed interval  $[t_k, t_{k+1}]$ .

In view of Lemma 5.2, the existence of a solution can be proved via inductive procedure: we define  $u(t)$  for  $t \in [0, T_s]$  by solving (2),(3) with initial state  $x(0)$ , defining thus the state trajectory  $x(t)$  for  $t \in [0, T_s]$ ; then, solve the OCP with  $x_1 = x(T_s)$  defining the solution on  $[T_s, 2T_s]$ , and so on.

<sup>3</sup>Proving or disproving the recursive feasibility it a highly non-trivial task even for convex MPC problems (Löfberg, 2012).

<sup>4</sup>Notice that we do not guarantee the uniqueness of a minimizer in each OCP. In some situations, e.g., where the plant is linear and  $\varkappa = 0$ , such a uniqueness is guaranteed by the strong convexity of the cost function. In practice, one has to choose the solution returned by the solver of TPBVP problems in use.

*Some remarks on validation of Assumption 5.1*

One class of systems satisfying Assumption 5.1 is constituted by systems whose right-hand side grows linearly in  $x$ . This is guaranteed by the following lemma.

**Lemma 5.3.** *Assumption 5.1 holds if  $U_C$  is bounded, the functions  $f, g$  satisfy Assumption 3.1, and the following condition is valid for some constants  $C_0, C_1 > 0$ :*

$$\forall x \in \mathbb{R}^{n_x} \quad \max\{\|f(x)\|, \|g(x)\|\} \leq C_0 + C_1\|x\|. \quad (29)$$

There are, however, many other situations where Assumption 5.1 can be validated despite violation of (29). Consider, for instance, the Lotka-Volterra model (22) considered in the positive orthant  $\mathbb{R}_+^2 = \{x : x_1, x_2 > 0\}$ . Rewriting (22) as

$$\begin{cases} \frac{d}{dt} \log x_1 = \alpha - \beta x_2 + u_1 \\ \frac{d}{dt} \log x_2 = \gamma x_1 - \delta + u_2, \end{cases} \quad (30)$$

one may easily notice that the set  $\mathbb{R}_+^2$  is forward invariant whenever  $u(t)$  is a locally bounded function. Indeed, if a solution  $x(\cdot)$  left  $\mathbb{R}_+^2$ , there would exist the first instant  $\tau > 0$  when  $\min(x_1(\tau), x_2(\tau)) = 0$ . Integrating (30) over  $[0, \tau)$  one proves, however, that functions  $\log x_i(t)$  remain bounded as  $t \rightarrow \tau$ , which leads to a contradiction. Similarly, (30) entails that all solutions starting at  $x_0 \in \mathbb{R}_+^2$  and corresponding to inputs  $u : [0, T] \rightarrow U_C$ , where  $U_C$  is from Assumption 3.2, are uniformly bounded on  $[0, T]$ . Indeed, the first equation in (30) implies

$$\log x_1(t) - \log x_1(0) \leq \bar{\chi}_1 := T(\alpha + u_{1,\max}) \quad \forall t \in [0, T].$$

Recalling that  $x_1(t) > 0$ , the second equation in (30) entails that

$$\underline{\chi}_2 := T(u_{2,\min} - \delta) \leq \log x_2(t) - \log x_2(0) \leq \bar{\chi}_2 := \gamma e^{\bar{\chi}_1} x_1(0) + T(u_{2,\max} - \delta).$$

Using the first equation, one proves that

$$\log x_1(t) - \log x_1(0) \geq \underline{\chi}_1 := T(\alpha + u_{1,\min} - e^{\bar{\chi}_2} x_2(0)).$$

Hence, Assumption 5.1 is valid for the Lotka-Volterra system, provided that only positive (and thus biologically feasible) initial conditions are considered.

## **5.2. Practical stability of the equilibrium**

In this subsection, we address a more difficult problem of *stability* of the NMPC scheme in question. Similar to the most of existing stability results, our criteria apply to the situation where the cost function penalizes the deviation of the system from a certain *equilibrium point*, that is,  $x_r$  and  $u_r$  satisfy the condition  $f(x_r) + g(x_r)u_r = 0$ , furthermore, the control effort  $u = u_r$  lies strictly inside the set  $U_C$ , that is, at the equilibrium point none of the actuators is saturated. Introducing the new state  $\tilde{x} = x - x_r$  and  $\tilde{u}$ , system (1) then can be rewritten as

$$\dot{\tilde{x}} = \tilde{f}(\tilde{x}) + \tilde{g}(\tilde{x})\tilde{u},$$

where the functions at the right-hand side are defined as

$$\tilde{f}(z) \doteq f(z + x_r) + g(z + x_r)u_r, \quad \tilde{g}(z) \doteq g(z + x_r).$$

Replacing  $f, g$  by  $\tilde{f}, \tilde{g}$  and  $U_C$  by  $\tilde{U}_C \doteq \{u - u_r : u \in U_C\}$  respectively, we henceforth adopt the following assumption.

**Assumption 5.4. (NMPC for equilibrium stabilization)** In (5) and (6), one has  $x_r = 0$  and  $u_r = 0$ . The pair  $x = 0, u = 0$  is an equilibrium of (1), that is,  $f(0) = 0$ . Finally,  $u_{i_{\min}} < 0 < u_{i_{\max}}$  for all  $i$ .

Furthermore, we will assume that the state constraints are neglected<sup>5</sup>, so  $\varkappa \equiv 0$ . Our stability analysis relies on the additional property of local controllability at zero, which requires to introduce a definition.

**Definition 5.5.** For given vectors  $x^0, x^* \in \mathbb{R}^{n_x}$ , set  $U_C \subset \mathbb{R}^{n_u}$  and time horizon  $T > 0$ , we say that state  $x^*$  is  $T$ -reachable from  $x^0$  with input constraint  $U_C$  if there exists a piecewise-continuous control  $u : [0, T] \rightarrow U_C$  such that the solution of (1) corresponding to  $u(\cdot)$  and emanating from  $x(0) = x^0$  arrives at  $x(T) = x^*$ . Let  $\mathcal{R}(x^*, T, U_C)$  denote the set of all initial conditions  $x^0$  from which  $x^*$  is  $T$ -reachable with input constraint  $U_C$ .

**Remark 4.** Denoting  $x^\dagger(t) = x(T - t)$ ,  $u^\dagger(t) = u(T - t)$ , where  $t \in [0, T]$ , it can be easily shown that

$$\dot{x}^\dagger(t) = -f(x^\dagger(t)) - g(x^\dagger(t))u^\dagger(t), \quad t \in [0, T]. \quad (31)$$

The set  $\mathcal{R}(x_0, T, U)$  is nothing else than the set of all possible  $x^\dagger(T)$  reachable from  $x_0$  under some signal  $u^\dagger : [0, T] \rightarrow U$ .

For brevity, let

$$\mathbf{B}_\varepsilon(x) \doteq \{x : \|x\| < \varepsilon\}, \quad \bar{\mathbf{B}}_\varepsilon(x) \doteq \{x : \|x\| \leq \varepsilon\}$$

stand for the open and closed ball of radius  $\varepsilon$  centered at 0.

**Assumption 5.6.** The equilibrium  $x = 0$  is an inner point of  $\mathcal{R}(0, T, U_C)$  for all  $T > 0, \varepsilon > 0$ , that is, for each  $\varepsilon > 0$  and  $T > 0$ , there exists  $\delta = \delta(\varepsilon, T)$  such that  $\mathbf{B}_\delta(0) \subseteq \mathcal{R}(0, T, U_C)$ .

Assumption 5.6 states, essentially, that, being close to equilibrium, one can reach the equilibrium in a short time, respecting the input constraint (as we will see, this trajectory also corresponds to a small value of the cost function). The property from Assumption 5.6 has a special name in the literature: If it holds, then it is said that the equilibrium is *small-time locally attainable* (Krastanov & Quincampoix, 2001). Introducing the time inverted dynamics (31), this assumption can be reformulated as the *small-time locally controllable* (STLC) at 0 with input constraint  $U_C$ . Analysis of STLC of nonlinear systems is currently a well-developed branch of nonlinear control that is currently beyond the scope of this manuscript, we refer the reader to recent

---

<sup>5</sup>Notice that if the optimal trajectories stay far from the boundary of the state constraint set  $X_C$ , then typically  $\varkappa(x(t)) \ll 1$ , and one can prove that the presence of penalty terms have small effect on the solution. We, however, omit the relevant analysis to keep things maximally simple.

works (Jafarpour, 2020; Krastanov, 2009; Krastanov & Quincampoix, 2001; Sarychev, 2006) and references therein. The simplest situation where STLC can be guaranteed is where the linearization at equilibrium  $(x, u) = (0, 0)$  is fully controllable (in the Kalman sense as an LTI system) (Sarychev, 2006); this condition, however, is violated in many nonlinear systems, e.g., controllability of rigid body dynamics typically requires more sophisticated tools of geometric control theory (Crouch, 1984). Another sufficient condition of STLC is the existence of a *feedback linearization*, which reduces the nonlinear plant to a controllable LTI system (Slotine & Li, 1990, Section 6.5).

### *Main results*

We are now ready to formulate our main results ensuring the stability of NMPC control scheme. For brevity, let

$$\mathcal{R}_0(T) \doteq \mathcal{R}(0, T, U_C).$$

Our first main result proves that, under sufficiently large terminal weight, the solutions starting sufficiently close to equilibrium, remain bounded. Namely, the set  $\mathcal{R}_0(T_p)$  is “weakly” invariant in the following sense.

**Theorem 5.7.** *Suppose that the input constraint set satisfies Assumption 3.2,  $X_C = \mathbb{R}^{n_x}$  and Assumptions 3.1, 5.4, 5.6 and are valid for the dynamical system (1). Suppose also that  $f, g$  satisfy the condition of linear growth (29). Let the integral cost be the function in (6) with some fixed matrices  $\mathbf{Q} = \mathbf{Q}^\top > 0$  and  $\mathbf{R} = \mathbf{R}^\top > 0$  and the terminal cost be given by (5). Then, a constant  $p_0$  exists such that for any matrix  $\mathbf{P} = \mathbf{P} > p_0 I$  the NMPC algorithm solving the receding horizon OCP (2),(3) provides the following properties of the closed-loop system:*

- (1) *the set  $\mathcal{R}_0(T_p)$  enjoys the following “invariance” property: if  $x(t_0) \in \mathcal{R}_0(T_p)$ , then  $x(t_k) \in \mathcal{R}_0(T_p)$  for all  $k$  (we are not claiming, however, that  $x(t)$  stays in  $\mathcal{R}_0(T_p)$  between sampling instants);*
- (2) *the solutions starting at  $\mathcal{R}_0(T_p)$  do not leave the larger set  $\mathcal{R}_0(T_p + T_S)$ , being thus uniformly bounded.*

Our next result, in fact, establishes a stronger fact. It appears that one can choose  $\mathbf{P}$  in such a way that all solutions starting in a  $\mathcal{R}_0(T_p)$ , are uniformly bounded and, furthermore, converge to a predefined neighborhood of the equilibrium. In this sense, we can make the NMPC *practically stable* in the set of initial conditions  $\mathcal{R}_0(T_p)$  by choosing the terminal weight large enough.

**Theorem 5.8.** *Let the assumptions of Theorem 5.7 be valid. Then, for each  $\varepsilon_* > 0$  there exist  $p_* = p_*(\varepsilon_*)$  such that whenever  $\mathbf{P} \geq p_* I$ , the NMPC provides additionally the ultimate boundedness of all solutions that emanate from  $\mathcal{R}_0(T_p)$  as follows*

$$\limsup_{t \rightarrow \infty} \|x(t)\| < \varepsilon_* \quad \forall x(0) \in \mathcal{R}_0(T_p). \quad (32)$$

**Remark 5.** It should be noted that, in fact, the weights  $p_0$  and  $p_*(\varepsilon)$ , for each  $\varepsilon > 0$  in Theorems 5.7 and 5.8 can be found explicitly, although the estimates are rather conservative.

**Remark 6.** In practice, the initial condition usually belongs to a known bounded

set  $\mathcal{D} \subset \mathbb{R}^{n_x}$ . Theorems 5.7 and 5.8 guarantee that, if  $T_p$  can be chosen so large that  $\mathcal{D} \subseteq \mathcal{R}_0(T_p)$ , one can always guarantee boundedness of the closed system’s trajectories by tuning the terminal weight  $\mathbf{P}$ . It should be noticed that various conditions of controllability, assuming explicitly or implicitly that the prediction horizon is large enough and the equilibrium is reachable from all possible initial conditions (respecting the input constraints), arise in all existing results on stability of MPC algorithms, see the discussion in our next subsection.

### *Discussion*

Stability of MPC algorithms is a classical problem, which is still far from being completely solved. We refer the reader to the recent monograph of Rawlings et al. (2022) and survey Mayne et al. (2000) that contain an overview of main historical milestones.

In general, even local stability of NMPC is *not* guaranteed as illustrated by the practical example from Raff et al. (2006). It was realized that the easiest way to ensure stability (local, asymptotic or practical) is to introduce a terminal constraint  $x(t_k + T_p) \in \Omega$ , where  $\Omega$  is some properly constrained set. Such “stabilizing” constraints appear in early works (Chen & Allgöwer, 1998; Mayne & Michalska, 1990; Michalska & Mayne, 1991, 1993). It should be noted that all of these works impose numerous assumptions on the plant or the cost function, e.g., continuity of the optimal control (Mayne & Michalska, 1990) (excluding thus bang-bang optimal control signals from consideration) or sufficiently small sampling time (Chen & Allgöwer, 1998).

This work continues another line of research that is concerned by removal the explicit constraint on  $x(t_k + T_p)$  and replacing it by a *terminal cost*, “pulling” the state vector to the equilibrium. The elimination of terminal constraints gives a number of advantages. In presence of such a constraint, the OCP is feasible *only* if the equilibrium (or its predefined neighborhood) is reachable from  $x(0)$  in time  $T_p$ , which leads to another sophisticated problem of tuning the prediction horizon. The terminal cost approach guarantees the feasibility of NMPC for an *arbitrary* initial condition if Assumption 5.1 holds (Lemma 5.2). Although formally stability is guaranteed only locally, in practice, often provides convergence to the equilibrium even if one does not know the minimal reachability time for  $x(0)$ . It should be noticed that the existing results on stability without terminal constraints yet in presence of terminal costs are mainly limited to discrete-time systems (Alamir, 2017; Grimm et al., 2005; Limon et al., 2006) and impose numerous restrictive assumptions on the nonlinear system, e.g., some results of Grimm et al. (2005) rely on the homogeneity of the system, whereas Limon et al. (2006) and Alamir (2017) assume the existence of special control Lyapunov functions that determine the performance index.

Finally, we would like to mention several works on “unconstrained” MPC, in particular, works by Grüne (2009), Reble & Allgöwer (2012), and more recent work by La et al. (2017), in which neither terminal cost nor terminal constraints are introduced, however, a *non-local* controllability condition (with an explicit estimate of the performance index on the solution leading from  $x(0)$  to 0) is imposed that assumes, essentially, the existence of some a priori estimate on the cost function as a function of  $x(0)$  and the prediction horizon  $T_p$  (which needs to be large enough to guarantee stability). Practical validation of the relevant conditions is a self-standing non-trivial problem.

## 6. Conclusion

In this work, we examine Nonlinear Model Predictive Control problems in presence of input constraints and, possibly, state constraints that are, however, relaxed by using (exterior) penalty functions. The contribution of this work is twofold. From the practical viewpoint, we show that the receding horizon optimal control problems can be efficiently solved via the Pontryagin Minimum Principle, turning the optimal control problem into a two-point boundary value problem. The resulting optimal input is then a function of the state and co-state variables, whose time evolution is described by the Hamiltonian equations. We provide a numerical example showing the applicability the efficiency of the control algorithm, showing excellent reference tracking and compliance with the input and path constraints.

The second contribution is theoretical and is concerned with practical stability of the NMPC algorithm in the problem of equilibrium stabilization. We show that introducing the terminal cost with a sufficiently large weight, one can provide local Lyapunov stability of the equilibrium and, furthermore, convergence of all solutions from a known bounded set to a predefined small ball.

Notice that, throughout the paper, we have assumed that the state vector is available. If this state is not completely measurable, an observer must be employed for inferring the system state from the output knowledge. However, using the observer substantially complicated analysis of stability; we leave the relevant analysis for future research. Another important direction is stability of non-equilibrium regimes, e.g., NMPC algorithms in problems of periodic reference tracking or geometric path following control.

### Author contributions

All the authors have equally contributed to the work.

### Financial disclosure

None reported.

### Disclosure statement

The authors declare no potential conflict of interests.

### Funding

M. Pagone is funded by the initiative “PNRRNextGenerationEU,” Mission 4, “Sustainable Mobility Center (Centro Nazionale per la Mobilità Sostenibile — CNMS),” Spoke n.2 — Sustainable road vehicle — with grant agreement no. CN 00000023. This manuscript reflects only the authors’ views and opinions, neither the European Union nor the European Commission can be considered responsible for them.

## References

- Ahmed, N. U., Wang, S. (2021). *Optimal Control of Dynamic Systems Driven by Vector Measures: Theory and Applications*. Springer.
- Alamir, M. (2017). Stability proof for nonlinear MPC design using monotonically increasing weighting profiles without terminal constraints. *Automatica*. 87, 455-459.
- Alcalá, E., Bessa, I., Puig, V., Sename, O., Palhares, R. (2022). MPC using an on-line TS fuzzy learning approach with application to autonomous driving. *Applied Soft Computing*. 130, 109698.
- Allgöwer, F., Findeisen, R., Nagy, Z. K. (2004). Nonlinear Model Predictive Control: From Theory to Application. *Journal of the Chinese Institute of Chemical Engineers*. Vol. 35, No. 3, 299-315.
- Boggio, M., Colangelo, L., Viridis, M., Pagone, M., Novara, C. (2022). Earth Gravity In-Orbit Sensing: MPC Formation Control Based on a Novel Constellation Model. *Remote Sensing*. 14(12), 2815.
- Boggio, M., Novara, C., Taragna, M. (2023). Trajectory planning and control for autonomous vehicles: a “fast” data-aided NMPC approach. *European Journal of Control*. Vol. 74, 100857.
- Boiroux, D., Jørgensen, J. B. (2019). Sequential  $\ell_1$  Quadratic Programming for Nonlinear Model Predictive Control. *IFAC PapersOnLine*. 52-1, 474-479.
- Bonnard, B., Faubourg, L., Launay, G., Trélat, E. (2003). Optimal control with state constraints and the space shuttle re-entry problem. *Journal of Dynamical and Control Systems*. Vol. 9., 155-199.
- Boumaza, H., Belarbi, K. (2022). Optimal model predictive control solution approximation using Takagi Sugeno for linear and a class of nonlinear systems International Journal of Dynamics and Control. Vol. 10, 1265-1278
- Bryson, A. E., Ho, Y. (1975). *Applied optimal control: optimization, estimation and control*. Taylor & Francis Inc.
- Cannon, M., Liao, W., Kouvaritakis, B. (2018). Efficient MPC Optimization using Potryagin’s Minimum Principle. *International Journal of Robust and Nonlinear Control*. 18:831-844.
- Chen, H., Allgöwer, F. (1998). A Quasi-Infinite Horizon Nonlinear Model Predictive Control Scheme with Guaranteed Stability. *Automatica*. Vol. 34, No. 10, 1205-1217.
- González Cisneros, P. S., Werner, H. (2020). Nonlinear model predictive control for models in quasi-linear parameter varying form. *International Journal of Robust and Nonlinear Control*. Vol. 30, 3945-3959.
- Coddington, E. A., Levinson, N. (1995). *Theory of ordinary differential equations*. McGraw-Hill, New York.
- Crouch, P. (1984). Spacecraft attitude control and stabilization: Applications of geometric control theory to rigid body models. *IEEE Transactions on Automatic Control*. 29(4): 321-331.
- Deng, H., Ohtsuka, T. (2019). A Parallel Newton-type method for nonlinear model predictive control. *Automatica*. 109, 108560.
- Deng, H., Ohtsuka, T. (2022). ParNMPC – a parallel optimisation toolkit for real-time nonlinear model predictive control. *International Journal of Control*. Vol. 95, No. 2, 390-405.
- Devia, C. A., Roa, M. C., Colorado, J., Patino, D. (2018). Towards a Nonlinear Model Predictive Control using the Extended Modal Series Method. *Proceedings of the European Control Conference*. June 12-15.
- Diehl, M., Bock, H. G., Diedam, H., Wieber, P.-B. (2006). Fast Direct Multiple Shooting Algorithms for Optimal Robot Control. In: Diehl, M., Mombaur, K. (eds) *Fast Motions in Biomechanics and Robotics*. Lecture Notes in Control and Information Sciences. Vol. 340, pp. 65-93.
- Dontchev, A. L., Kolmanovskiy, I. V., Krastanov, M. I., Veliov, V. M., Voung, P. T. (2020). Approximating optimal finite horizon feedback by model predictive control. *System & Control Letters*. 139, 104666.
- Dragomir, S. S. (2003). *Some Gronwall Type Inequalities and Applications*. Nova Science Pub-

- lishers.
- Dubljevic, S., Humaloja, J. (2020). Model predictive control for regular linear systems. *Automatica*. 119 (2020) 109066.
- Graichen, K., Petit, N. (2009). Incorporating a class of constraints into the dynamics of optimal control problems. *Optimal Control Applications and Methods*. Vol. 30, Issue 6, pp. 537-561.
- Graichen, K., Kugi, A., Petit, N., Chaplais, F. (2010). Handling constraints in optimal control with saturation functions and system extension. *Systems & Control Letters*. 59(11): 671-679
- Grancharova, A., Johansen, T.A. (2012). Explicit Nonlinear Model Predictive Control. Theory and Applications. Lecture Notes in Control and Information Sciences, vol. 429, Springer.
- Grimm, G., Messina, M. J., Tuna, S. E., Teel, A. R. (2005). Model Predictive Control: For Want of a Local Control Lyapunov Function, All is Not Lost. *IEEE Transaction on Automatic Control*. Vol. 50, No. 5.
- Gros, S., Zanon, M., Quirynen, R., Bemporad, A., Diehl, M. (2020). From linear to nonlinear MPC: bridging the gap via the real-time iteration. *International Journal of Control*. Vol. 93, No. 1, 62-60.
- Grüne, L. (2009). Analysis and design of unconstrained nonlinear MPC schemes for finite and infinite dimensional systems. *SIAM Journal on Control and Optimization*. 48(2): 1206-1228.
- Guerrero-Fernandez, J. L., González-Villareal, O. J., Rossiter, J. A. (2023). Efficiency-aware nonlinear model-predictive control with real-time iteration scheme for wave energy converters. *International Journal of Control*. Vol. 96, No. 8, 1909-1921
- Ha, S.N. A Nonlinear Shooting Method for Two-Point Boundary Value Problems (2001). *Computers and Mathematics with Applications* Vol. 42, 1411-1420
- Hauser, J., Saccon, A. (2006). A Barrier Function Method for the Optimization of Trajectory Functionals with Constraints. *Proceedings of the 45th IEEE Conference on Decision & Control*. December 13-15.
- Jafarpour, S. (2020). On small-time local controllability. *SIAM Journal on Control and Optimization*. 58(1): 425-446.
- Kierzenka, J., Shampine, L. F. (2001). A BVP solver based on residual control and the Matlab PSE, *ACM Trans. Math. Softw.* 40, 299-316.
- Kovaltchouk, T., Rongère, F., Primot, M., Aubry, J., Ahmed, H. B, Multon, B. (2015). Model Predictive Control of a Direct Wave Energy Converter Constrained by the Electrical Chain Using an Energetic Approach. *Proceedings of the European Wave and Tidal Energy Conference*.
- Krastanov, M. (2009). A sufficient condition for small-time local controllability. *SIAM Journal on Control and Optimization*. 48(4): 2296-2322.
- Krastanov, M., Quincampoix, M. (2001). Local small time controllability and attainability of a set for nonlinear control system. *ESAIM: Control, Optimisation and Calculus of Variations*. 6, 499-516.
- Kvikto, A. N. (2020). Solution of the local boundary value problem for a nonlinear non-stationary system in the class of synthesising controls with account of perturbations. *International Journal of Control*. Vol. 93, No. 8, 1931-1941.
- La, H. C., Potschka, A., Bock, H. G. (2017). Partial stability for nonlinear model predictive control. *Automatica*. 78, 14-19.
- Lagarias, J. C., Reeds, J. A, Wright, M. H, Wright, P. E. (1998). Convergence Properties of the Nelder-Mead Simplex Method in Low Dimensions. *SIAM Journal of Optimization*. Vol. 9, no. 1, pp. 112-147.
- Limón, D., Alamo, T., Salas, F., Camacho, E. F. (2006) On the Stability of Constrained MPC Without Terminal Constraint, *IEEE Transactions on Automatic Control*. Vol. 51, no.5, pp. 832-836.
- Löfberg, L. (2012). Oops! I cannot do it again: Testing for recursive feasibility in MPC. *Automatica*. 48(3): 550-555.
- Malisani, P., Chaplais, F., Petit, N. (2016). An interior penalty method for optimal control problems with state and input constraints of nonlinear systems. *Optimal Control Applications and Methods*. Vol. 37, Issue 1, pp 3-33.

- Mayne, D. Q., Michalska, H. (1990). Receding Horizon Control of Nonlinear Systems. *IEEE Transaction of Automatic Control*. Vol. 35, No. 7, July 1990.
- Mayne, D. Q., Rawlings, J. B., Rao, C. V., Scokaert, P. O. M. (2000). Constrained model predictive control: Stability and optimality. *Automatica*. 36: 789-814.
- Mendes, T.P.G, Schnitman, L., Nogueira, I.B.R., Almeida Peixoto Ribeiro, A.M., Rodrigues, A.E., Loureiro, J.M., Martins, M.A.F.(2022). A new Takagi-Sugeno-Kang model-based stabilizing explicit MPC formulation: An experimental case study with implementation embedded in a PLC. *Expert Systems With Applications*. Vol. 210, p. 118369
- Michalska, H., Mayne, D. Q. (1991) Receding Horizon control of nonlinear systems without differentiability of the optimal value function. *System & Control Letters*. 16, 123-130.
- Michalska, H., Mayne, D. Q. (1993). Robust receding horizon control of constrained nonlinear systems. *IEEE Transaction on Automatic Control*. AC-38(11), 1623-1633.
- Okawa, I., Nonaka, K. (2021). Linear complementarity model predictive control with limited iterations for box-constrained problems. *Automatica*. 125, 109429.
- Ohtsuka, T., Fujii, H. (1997). Real-time Optimization Algorithm for Nonlinear Receding-horizon Control. *Automatica*. Vol. 33, No. 6, pp. 1147-1154.
- Ohtsuka, T. (2003). A continuation/GMRES method for fast computation of nonlinear receding horizon control. *Automatica*. 40 (2004) 563-574.
- Pagone, M., Boggio, M., Novara, C., Proskurnikov, A., Calafiore, G. C. (2022). A penalty function approach to constrained Pontryagin-based Nonlinear Model Predictive Control. *Proceedings of the 61th IEEE Conference on Decision and Control*. December 6-9, Cancun, Mexico.
- Pesch, H. A practical guide to the solution of real-life optimal control problems. (1994) *Control and Cybernetics*. Vol. 23, pp. 7-60.
- Raff, T., Huber, S., Nagy, Z. K., Allgower, F. (2006). Nonlinear model predictive control of a four tank system: An experimental stability study. *IEEE International Conference on Control Applications*. pp. 237-242
- Rawlings, J. B., Mayne, D. Q., Diehl, M. M. (2022). *Model Predictive Control: Theory, Computation, and Design*, Nob Hill Publishing LLC, 2022.
- Reble, M., Allgöwer, F. (2012). Unconstrained model predictive control and suboptimality estimates for nonlinear continuous-time systems. *Automatica*. 48, 1812-1817.
- Sarychev, A. (2006). Lie extensions of nonlinear control systems. *Journal of Mathematical Sciences*. 135(4): 3195–3233.
- Shampine, L., Gladwell, I., Thompson, S. (2003). *Solving ODEs with MATLAB*. Cambridge: Cambridge University Press. 2003.
- Slotine, J. J., Li, W. (1990). *Applied Nonlinear Control*. Pearson Education, US.
- Suwartadi, E., Krogstad, S., Foss, B. (2010). A Lagrangian-Barrier Function for Adjoint State Constraints Optimization of Oil Reservoirs Water Flooding. *Proceedings of the 49th Conference on Decision & Control*. December 15-17.
- Tøndel, P., Johansen, T.A., Bemporad, A. (2003a) An algorithm for multi-parametric quadratic programming and explicit MPC solutions. *Automatica* 39, 489–497
- Tøndel, P., Johansen, T.A., Bemporad, A. (2003b) Evaluation of piecewise affine control via binary search tree. *Automatica* 39, 945-950
- Vidano, S., Novara, C., Pagone, M., Grzymisch, J. (2022). The LISA DFACS: Model Predictive Control design fo the test mass release phase. *Acta Astronautica*. Vol. 193, pp. 731-743.
- Wang, C., Ma, C., Zhou, J. (2014). A new class of exact penalty functions and penalty algorithms. *Journal of Global Optimization*. 58:51-73.
- Wang, Z., Li, Y. (2007). Indirect method for inequality constrained optimal control problems. *IFAC PapersOnLine*. 50-1, 4070-4075.
- Zhang, Y., Yan, X., Liao, B., Zhang, Y., Ding, Y. (2016). Z-type control of populations for Lotka-Volterra model with exponential convergence. *Mathematical Biosciences*. 272, 15-23.

## Appendix A. Proof of Lemma 5.2

Throughout this subsection, we assume that the assumptions of Lemma 5.2 hold, i.e.,  $f, g, \varkappa$  are  $C^1$ -smooth, Assumption 5.1 holds and the terminal cost is given by (5).

**Step 1.** We first prove that for each  $x_0 \in \mathbb{R}^{n_x}$  the OCP has a solution:

$$\begin{aligned}
 \text{minimize} \quad & \tilde{J} = \phi(\hat{x}(T_p)) + \int_0^{T_p} \Phi(\hat{x}(\tau), \hat{u}(\tau)) + \varkappa(\hat{x}(\tau)) \, d\tau \\
 \text{subject to constraints} \quad & \\
 & \dot{\hat{x}}(\tau) = f(\hat{x}(\tau)) + g(\hat{x}(\tau))\hat{u}(\tau), \quad \hat{x}(0) = x_0 \\
 & \hat{x}(\tau) \in X_C \subset \mathbb{R}^{n_x}, \quad \hat{u}(\tau) \in U_C \subset \mathbb{R}^{n_u}, \quad \forall \tau \in [0, T_p],
 \end{aligned} \tag{A1}$$

This is entailed by the standard existence result of optimal control theory, established as Theorem 4.2.4 Ahmed & Wang (2021), applied in the special situation where the integrand  $\tilde{\Phi}(x, u) = \Phi(x, u) + \varkappa(x)$  and the terminal cost are time-invariant and nonnegative. Although Ahmed & Wang (2021) adopt some technical assumptions that are not supposed to hold (such as, e.g., the global Lipschitz condition on  $f, g$  and the constraint (29)), the analysis of the proof reveals that it the following key conditions are sufficient to prove the solution existence:

- (a) each Lebesgue measurable function  $\hat{u} : [0, T_p] \rightarrow U_C$  corresponds to an admissible solution  $(\hat{x}, \hat{u})$ ;
- (b) the state vectors  $\hat{x}(\cdot) : [0, T_p] \rightarrow \mathbb{R}^{n_x}$  constitute a precompact set in the space of all continuous functions  $C([0, T_p] \rightarrow \mathbb{R}^{n_x})$ ; thanks to the Arzelá-Ascoli theorem, this holds when the state variables  $\hat{x}(\cdot)$  of all admissible solutions and their derivatives  $\dot{\hat{x}}(\cdot)$  are uniformly bounded;
- (c)  $f$  and  $g$  are Lipschitz continuous on the bounded set, containing all admissible solutions;
- (d) for all  $\hat{x} \in \mathbb{R}^{n_x}$ , the ‘‘contingent set’’

$$Q(\hat{x}) = \{(\xi, \eta) \in \mathbb{R} \times \mathbb{R}^{n_x} : \xi \geq \tilde{\Phi}(\hat{x}, \hat{u}), \eta = f(\hat{x}) + g(\hat{x})\hat{u} \text{ for some } \hat{u} \in U_C\}$$

is closed and convex; also,  $Q$  is semi-continuous as a multi-valued function of  $\hat{x}$ .

Conditions (a)-(c) are ensured by boundedness of  $U_C$  and Assumption 5.1. Each Lebesgue measurable function  $\hat{u} : [0, T_p] \rightarrow U_C$  corresponds to an admissible solution  $(\hat{x}, \hat{u})$ , which entails (a). The state variables of all admissible solutions stay in some ball  $\hat{x}(t) \in \mathbf{B}_R$ , where  $R > 0$  is a known constant. In view of (1) and boundedness of  $U_C$ , the derivatives of all admissible solutions are thus also uniformly bounded, so the set of state functions  $\{\hat{x}(\cdot)\}$  is precompact in  $C([0, T_p] \rightarrow \mathbb{R}^{n_x})$ . This proves (b). Finally,  $f$  and  $g$  are  $C^1$ , being thus Lipschitz on the ball  $\mathbf{B}_R$ , so condition (c) is satisfied.

To prove (d), we first show the convexity of  $Q(\hat{x})$ . Indeed, choosing  $(\xi_1, \eta_1) \in Q(\hat{x})$  and  $(\xi_2, \eta_2) \in Q(\hat{x})$ , one can find  $\hat{u}_1, \hat{u}_2 \in U_C$  such that  $\eta_i = f(\hat{x}) + g(\hat{x})\hat{u}_i$  and  $\xi_i \geq \tilde{\Phi}(\hat{x}, \hat{u}_i)$  for  $i = 1, 2$ . For an arbitrary  $a \in [0, 1]$ ,

$$\begin{aligned}
 a\eta_1 + (1-a)\eta_2 &= f(\hat{x}) + g(\hat{x})(a\hat{u}_1 + (1-a)\hat{u}_2), \\
 a\xi_1 + (1-a)\xi_2 &\geq a\tilde{\Phi}(\hat{x}, \hat{u}_1) + (1-a)\tilde{\Phi}(\hat{x}, \hat{u}_2) \geq \tilde{\Phi}(\hat{x}, a\hat{u}_1 + (1-a)\hat{u}_2),
 \end{aligned}$$

entailing that  $a(\xi_1, \eta_1) + (1-a)(\xi_2, \eta_2) \in Q(\hat{x})$ . Here we use the convexity of  $\tilde{\Phi}(\hat{x}, \cdot)$

defined by (6).

To prove that  $Q(\hat{x})$  is closed, consider some sequence  $(\xi_k, \eta_k) \in Q(\hat{x})$  converging to  $(\xi_*, \eta_*) \in \mathbb{R} \times \mathbb{R}^{n_x}$ . Let  $\hat{u}_k \in U_C$  be such that

$$\xi_k \geq \hat{\Phi}(\hat{x}, \hat{u}_k), \quad \eta_k = f(\hat{x}) + g(\hat{x})\hat{u}_k$$

Since  $U_C$  is a compact set, without loss of generality one may assume that  $\hat{u}_k \rightarrow \hat{u}_* \in U_C$  as  $k \rightarrow \infty$ . Passing to the limit, one has

$$\xi_* \geq \hat{\Phi}(\hat{x}, \hat{u}_*), \quad \eta_* = f(\hat{x}) + g(\hat{x})\hat{u}_*$$

which means that  $(\xi_*, \eta_*) \in Q(\hat{x})$ . The upper-semicontinuity is proved similarly by using the continuity of all  $\hat{\Phi}, f, g$ . We omit the proof for the sake of brevity.

**Step 2.** The statement of Lemma 5.2 can now be proved via induction on  $k = 0, 1, \dots$ . Indeed, we know that the OCP (A1) has a solution for a given  $x_0 = x(0)$ . Applying the initial segment of optimal control  $u(t) = \hat{u}^*|_{[0, t_1]}$ , the solution  $x = \hat{x}^*|_{[0, t_1]}$  is well defined for  $t \in [0, t_k]$ . Now, since the system (1) and the cost function are time-invariant, the OCP with cost function  $\hat{J}$  and constraints (3) at time  $t_1 = T_S$  becomes equivalent to (A1) (where  $x_0 = x(t_1)$ ) after time shift  $t \mapsto t - t_1$ , admitting thus an optimal solution, which allows to define the state vector on  $[t_1, t_2]$ , and so on, the OCP at time  $t_k$  is equivalent to (A1) (where  $x_0 = x(t_k)$ ) and uniquely determines the state vector on  $[t_k, t_{k+1}]$ . This finishes the proof of the lemma.

## Appendix B. Proof of Lemma 5.3 and additional corollaries

In the proof of our results, we will use the following simplified form of Gronwall lemma (Dragomir, 2003, Corollary 3).

**Proposition B.1.** (*Gronwall lemma*) *Let  $\chi : [t_0, t_1] \rightarrow \mathbf{R}$  be a nonnegative measurable function and  $c \in \mathbb{R}$  be constant. Then, every function  $\xi(t)$  satisfying the inequality*

$$\xi(t) \leq c + \int_{t_0}^t \chi(s)\xi(s)ds \quad \forall t \in [t_0, t_1]$$

*admits the following upper bound*

$$\xi(t) \leq c \exp\left(\int_{t_0}^t \chi(s) ds\right) \quad \forall t \in [t_0, t_1].$$

Lemma 5.3 is now straightforward from the following simple corollary, which gives an explicit estimate of the state trajectories emanating from  $x_0$  and corresponding to the input  $u : [0, T] \rightarrow U_C$ .

**Corollary B.2.** *Let the system (1) obey Assumptions 3.1 and (29),  $T > 0$  and  $u : [0, T] \rightarrow U$  be a Lebesgue measurable input signal, attain its values in a bounded set  $U$ . Then, the solution of the Cauchy problem*

$$\dot{x}(t) = f(x(t)) + g(x(t))u(t), \quad x(0) = x_0$$

is well-defined on  $[0, T]$  and admits the following upper bound

$$\|x(t)\| \leq (\|x_0\| + C_0KT)e^{C_1Kt}, \quad K \doteq 1 + \sup_{u \in U} \|u\|.$$

Here  $C_0, C_1$  are constants from (29).

**Proof.** The local existence and uniqueness of the solution is implied by the standard Carathéodory theorem and (local) Lipschitz property of  $f$  and  $g$  (Coddington & Levinson, 1955, Chapter 2). Assuming that the solution is well-defined on some interval  $[0, t_0)$ , one has

$$\begin{aligned} \|x(t)\| - \|x(0)\| &\leq \|x(t) - x(0)\| = \\ &= \left\| \int_0^t f(x(s)) + g(x(s))u(s) ds \right\| \leq C_0KT + \int_0^t KC_1\|x(s)\| ds. \end{aligned}$$

the latter inequality is entailed by the inequality  $\|f(x(t)) + g(x(t))u(t)\| \leq K(C_0 + C_1\|x(t)\|)$  and  $t \leq T$ . The statement is now straightforward from the Gronwall lemma. Hence,  $\|x(t)\| \leq (\|x_0\| + C_0KT)e^{C_1Kt}$  for all  $t$  where the solution exists. It remains to notice that the interval of its existence coincides with  $[0, T]$ , because the state vector's norm remains bounded as  $t \leq T$ .  $\square$

Corollary B.2 can be reformulated for the time inverted dynamics (31), leading to the following statement.

**Corollary B.3.** *Let the system (1) obey Assumptions 3.1 and condition (29). Then for each  $x_0 \in \mathbb{R}^{n_x}$ ,  $T > 0$  and bounded set  $U \subseteq \mathbb{R}^{n_u}$  the set  $\mathcal{R}(x_0, T, U)$  introduced in Definition 5.5 is bounded:*

$$\|x\| \leq (\|x_0\| + C_0KT)e^{C_1KT} \quad \forall x \in \mathcal{R}(x_0, T, U),$$

where constants  $C_0, C_1, K$  are same as in Corollary B.2.

**Proof.** Since  $x^\dagger(t) = x(T - t)$ ,  $u^\dagger(t) = u(T - t)$ , where  $t \in [0, T]$ , are solutions of the system (31), the set  $\mathcal{R}(x_0, T, U)$  is nothing else than the set of all possible  $x^\dagger(T)$  reachable from  $x_0$  under some signal  $u^\dagger : [0, T] \rightarrow U$ . Obviously, system (31) obeys the assumptions of Corollary B.2, the state vectors from  $\mathcal{R}(x_0, T, U)$  admit the same bound as derived in the latter Corollary.  $\square$

## Appendix C. Uniform boundedness and convergence of the solutions

In this section, we prove Theorems 5.7 and 5.8. The proof will exploit the standard ‘‘Lyapunov-type’’ function  $V$ , defined as the optimal value in the OCP. Note that in our framework,  $V$  is not a true Lyapunov function, since it need not decrease along the system's trajectories. However, some weaker Lyapunov property will be sufficient to establish the practical stability.

Henceforth, we assume that all assumptions of Theorem 5.7 are valid, in particular,  $(x_r, u_r) = (0, 0)$  is an equilibrium and  $\varkappa(x) \equiv 0$ . We also adopt, without loss of

generality<sup>6</sup>, the following simplifying assumption that can always be provided by a linear change of variables.

**Standing Assumption:** The weight matrices of state and control “energy” in (6) are identity  $\mathbf{Q} = I_{n_x}$  and  $\mathbf{R} = I_{n_u}$ . Hence, only one parameter determining the properties of NMPC is the terminal weight matrix  $\mathbf{P}$ , which will be chosen large enough.

**Definition C.1.** Let  $V_{\mathbf{P}}(x_0)$  be the minimum value<sup>7</sup> in the following OCP

$$\mathbf{OCP}(T_0, x_0) \quad \left\{ \begin{array}{l} \text{minimize } J_{\mathbf{P}} = \hat{x}(T_p + T_0)^\top \mathbf{P} \hat{x}(T_p + T_0) + \\ \quad + \int_{T_0}^{T_0 + T_p} \Phi(\hat{x}(\tau), \hat{u}(\tau)) \, d\tau \quad \text{subject to constraints} \\ \hat{\dot{x}}(\tau) = f(\hat{x}(\tau)) + g(\hat{x}(\tau))\hat{u}(\tau), \quad \hat{x}(T_0) = x_0 \\ \hat{x}(\tau) \in X_C \subset \mathbb{R}^{n_x}, \quad \hat{u}(\tau) \in U_C \subset \mathbb{R}^{n_u}, \quad \forall \tau \in [T_0, T_0 + T_p], \end{array} \right. \quad (\text{C1})$$

where  $\Phi(\hat{x}(\tau), \hat{u}(\tau)) = \|\hat{x}\|^2 + \|\hat{u}\|^2$ .

Obviously, problem  $\mathbf{OCP}(T_0, x_0)$  with an arbitrary  $T_0$  reduces to  $\mathbf{OCP}(0, x_0)$  by means of the time shift, for this reason,  $V_{\mathbf{P}}(x_0)$  does not depend on  $T_0$ . One also notices that the receding horizon  $\mathbf{OCP}$  (2), (3) is nothing else than  $\mathbf{OCP}(t_k, x(t_k))$ .

### C.1. Properties of reachability sets and upper estimates on $V_{\mathbf{P}}$ .

To prove the first statement of Theorem 5.7, some simple statements about the reachability sets. The first property is straightforward from the definition of reachability sets.

**Proposition C.2.** *If  $x^1 \in \mathcal{R}(x^0, T, U)$  and  $x^2 \in \mathcal{R}(x^1, T', U)$ , then  $x^2 \in \mathcal{R}(x_0, T + T', U)$*

**Proof.** The control input  $u : [0, T + T'] \rightarrow U$  driving the state trajectory from  $x_2$  to  $x_0$  is found as the concatenation of two signals

$$u(t) = \begin{cases} u^2(t), & t \in [0, T'], \\ u^1(t - T'), & t \in [T', T + T'], \end{cases}$$

where  $u^1 : [0, T] \rightarrow U$  brings the state from  $x^1$  to  $x^0$  and  $u^2 : [0, T'] \rightarrow U$  drives the state from  $x^2$  to  $x^1$ .  $\square$

For brevity, denote

$$\mathcal{R}_0(T) \doteq \mathcal{R}(0, T, U_C).$$

**Corollary C.3.** *The sets  $\mathcal{R}_0(T)$  are nested, that is,  $\mathcal{R}_0(T) \subseteq \mathcal{R}_0(T')$  when  $T \leq T'$ .*

**Proof.** The proof is immediate from Proposition C.2 by noticing that  $0 \in \mathcal{R}_0(T' - T)$  (applying the input  $u = 0$ , one can keep the system at equilibrium  $x = 0$  thanks to Assumption 5.4).  $\square$

<sup>6</sup>One can always get rid of weight matrices by a linear change of variables.

<sup>7</sup>Recall that the minimum exists in view of Lemma 5.2

Given  $T > 0$  and  $x_0 \in \mathcal{R}_0(T)$ , let  $u_{T,x_0} : [0, T] \rightarrow U_C$  the control input driving the state trajectory from  $x_0$  to 0 in time  $T$  and  $x_{T,x_0} : [0, T] \rightarrow \mathbb{R}^{n_x}$  stand for the corresponding state trajectory.

**Corollary C.4.** *The state  $x_{T,x_0}(t)$  belongs to  $\mathcal{R}_0(T)$  for all  $T > 0$ ,  $x_0 \in \mathcal{R}_0(T)$ .*

**Proof.** Obviously, from state  $x_* = x_{T,x_0}(t_*)$ , where  $t_* \in (0, T]$  the equilibrium  $x = 0$  can be reached in time  $T - t_*$  by applying the truncated control input  $u_{T-t_*,x_*}(t) = u_{T,x_0}(t + t_*)$ , where  $t \in [0, T - t_*]$ . Hence,  $x_* \in \mathcal{R}_0(T - t_*) \subseteq \mathcal{R}_0(T)$ .  $\square$

**Corollary C.5.** *The following supremum is finite*

$$S \doteq \sup \left\{ V_{\mathbf{P}}(x_0) : \mathbf{P} = \mathbf{P}^\top \geq 0, x_0 \in \mathcal{R}_0(T_p) \right\} < \infty.$$

**Proof.** For each  $x_0 \in \mathcal{R}_0(T_p)$ , the functions  $\hat{x} = x_{T_p,x_0}$  and  $\hat{u} = u_{T_p,x_0}$  satisfy all constraints in (C1). Furthermore, we know that  $\hat{x}(t) \in \mathcal{R}_0(T_p)$  for all  $t \in [0, T]$  and, finally,  $\hat{x}(T) = 0$ , so the terminal cost is null on  $\hat{x}$ . Since Assumption 5.1 holds for the inverted dynamics (31),  $\hat{x}(t)$  is uniformly bounded, also,  $\hat{u}(t) \in U_C$  is also bounded. It remains to notice that

$$0 \leq V_{\mathbf{P}}(x_0) \leq \int_0^{T_p} \Phi(\hat{x}(t), \hat{u}(t)) dt,$$

where the right-hand side *does not depend* on  $\mathbf{P}$  and is bounded uniformly over all  $x_0 \in \mathcal{R}_0(T_p)$ .  $\square$

The following final corollary will be used later in the proof of Theorem 5.8.

**Corollary C.6.** *The function  $V_{\mathbf{P}}(x_0)$  converges to 0 as  $x_0 \rightarrow 0$ , and this convergence is uniform in  $\mathbf{P}$ .*

**Proof.** According to Assumption 5.6, as  $\|x_0\|$  becomes small enough, the equilibrium  $x = 0$  is reachable from 0 in time  $T \leq T_p$ , which can be arbitrarily small. Assuming that  $x_0 \in \mathcal{R}_0(T)$ , one has  $x_{T,x_0}(t) \in \mathcal{R}_0(T)$  for each  $t$ , and hence, in view of Corollary B.3, one has  $\|x_{T,x_0}(t)\| \leq c(T)$ , where  $c(T)$  is some continuous function of  $T$ . The pair of functions

$$\hat{x}(t) = \begin{cases} x_{T,x_0}(t), & t \in [0, T], \\ 0 & t \in [T, T_p], \end{cases} \quad \hat{u}(t) = \begin{cases} u_{T,x_0}(t), & t \in [0, T], \\ 0 & t \in [T, T_p] \end{cases}$$

then satisfies all constraints in (C1), and hence

$$V_{\mathbf{P}}(x_0) = \int_0^{T_p} \Phi(\hat{x}(t), \hat{u}(t)) dt = \int_0^T \Phi(\hat{x}(t), \hat{u}(t)) dt \leq \tilde{c}(T) \doteq T \left( c(T) + \max_{u \in U_C} \|u\|^2 \right). \quad (\text{C2})$$

Note that  $\tilde{c}(T)$  vanishes as  $T \rightarrow 0$ . Choosing  $\delta > 0$  small enough, one can thus provide that the reachability time  $T = T(\delta)$  is small for all  $x_0 \in \mathbf{B}_\delta$  (Assumption 5.6), and hence  $V_{\mathbf{P}}(x_0)$  can also be done smaller than any predefined number  $\varepsilon > 0$  independent of the choice of  $\mathbf{P}$ .  $\square$

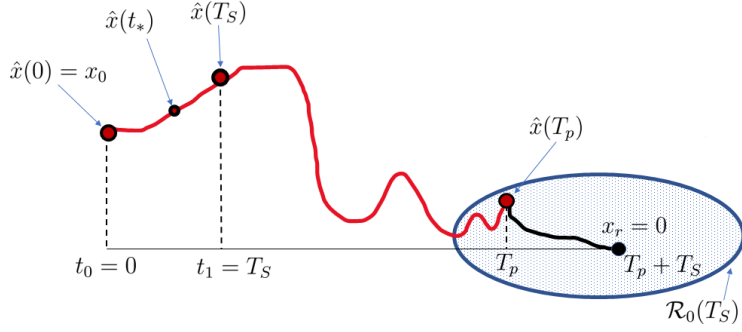


**Figure C1.** Illustration to the proof of Theorem 5.7. The red curve is the optimal state trajectory in (A1), the black curve is an arbitrary state trajectory reaching 0 in time  $T_S$  (under some admissible input).

### C.2. Proof of Theorem 5.7

The proof of first statement (i) relies on Corollary C.5 and Assumption 5.6. In view of Assumption 5.6, the set  $\mathcal{R}_0(T_S) = \mathcal{R}(0, T_S, U_C)$  contains a sufficiently small ball  $\mathbf{B}_\delta$ . Choose now  $p_0 = S/\delta^2$ , where  $S$  is the constant from Corollary C.5 and suppose that  $\mathbf{P} \geq p_0 I$ . Then, considering the optimal control problem (A1), one shows that the *optimal* trajectory  $\hat{x}$  starting at  $\hat{x}(0) \in \mathcal{R}_0(T_p) \setminus \{0\}$ , arrives at a point  $\hat{x}(T_p)$  such that

$$\|\hat{x}(T_p)\|^2 \leq \frac{1}{p_0} \hat{x}(T_p)^\top \mathbf{P} \hat{x}(T_p) < \frac{1}{p_0} V_{\mathbf{P}}(\hat{x}(0)) \leq \frac{S}{p_0} \leq \delta^2.$$

Obviously, the optimal trajectory starting at  $\hat{x}(0) = 0$  remains at the equilibrium, so the inequality is also valid. Hence, the equilibrium is  $T_S$ -reachable from  $\hat{x}(T_p) \in \mathbf{B}_\delta$ . Since we reach  $\hat{x}(T_p)$  from  $\hat{x}(T_S)$  in time  $T_p - T_S$  under the optimal control  $\hat{u}|_{[T_S, T_p]}$ , the equilibrium is  $T_p$ -reachable also from  $\hat{x}(T_S)$  (Proposition C.2). For the same reason, from  $\hat{x}(t_*)$ , where  $t_* \in (0, T_S)$ , the equilibrium is reachable in time  $T_p + T_S - t_* \leq T_p + T_S$ . This is illustrated in Fig. C1.

In view of Corollary C.3, the optimal trajectory cannot leave the set  $\mathcal{R}_0(T_S + T_p)$ , which is bounded (Corollary B.3).

The statement of Theorem 5.7 is now straightforward. Recall that the solution  $x(t), u(t)$  of the closed-loop system on interval  $[0, t_1] = [0, T_S]$  is coincident with the optimal trajectory in  $\mathbf{OCP}(0, x(0))$ . Hence, if  $x(0) \in \mathcal{R}(T_p)$  and  $\mathbf{P} \geq p_0 I$ , then  $x(t_1) \in \mathcal{R}(T_p)$ . Applying the same argument to  $\mathbf{OCP}(t_1, x(t_1))$ , one proves that  $x(t_2) \in \mathcal{R}(T_p)$ , and so on; the induction on  $k$  proves easily that  $x(t_k) \in \mathcal{R}(T_p)$  for all  $k$ . Similarly, for each  $t_* \in (0, t_1)$ , we have  $x(t_*) = \hat{x}(t_*) \in \mathcal{R}_0(T_S + T_p)$ , which statement, using induction on  $k$ , can thus be proved for all  $t_* \in (t_k, t_{k+1})$ , which finishes the proof.  $\square$

### C.3. Two additional properties of the function $V_{\mathbf{P}}$

In this technical subsection, we further develop Theorem 5.7 and establish two important properties of  $V_{\mathbf{P}}$  on the set  $\mathcal{R}_0(T_p)$ .

*A lower estimate on the function  $V_{\mathbf{P}}$*

To prove Theorem 5.8, we will need the strict positive definiteness of the function  $V_{\mathbf{P}}$ , which is enabled by Theorem 5.7 and is established by Corollary C.8 below. We start with proving the following proposition.

**Proposition C.7.** *Consider the auxiliary integral functional*

$$\Psi(x, u) = \int_0^{T_S} \Phi(x(\tau), u(\tau)) d\tau,$$

where  $x(t), u(t)$  is some solution to (1) (possibly, violating the constraint  $u(t) \in U_C$ ), defined at least on  $[0, T_S]$ , and  $\Phi$  is same as in (C1). Then, for each bounded set  $\mathcal{D} \subset \mathbb{R}^{n_x}$  a constant  $M = M(\mathcal{D})$  exists such that

$$\|x(0)\|^2 \leq M\Psi(x, u) \tag{C3}$$

for any solution  $x, u$  such that  $x(t) \in \mathcal{D}$  for all  $t \in T_S$ .

**Proof.** In view of Assumption 3.1, the function  $f$  is Lipschitz on the bounded set  $\mathcal{D}$ , in particular,  $|x^\top f(x)| \leq \mathcal{C}_1 \|x\|^2$  for all  $x \in \mathcal{D}$ . The continuous function  $x^\top g(x)$  is bounded on  $\mathcal{D}$ , in particular,  $\|g(x)\| \leq \mathcal{C}_2$  for all  $x \in \mathcal{D}$ , and

$$|x^\top g(x)u| \leq \frac{1}{2} (\|x\|^2 + \|g(x)\|^2 \|u\|^2).$$

Choosing  $\mathcal{C} = \max\{\mathcal{C}_1 + 1/2, \mathcal{C}_2^2\}$ , one thus proves that

$$\left| x^\top (f(x) + g(x)u) \right| \leq \mathcal{C} (\|x\|^2 + \|u\|^2) \quad \forall x \in \mathcal{D}, u \in \mathbb{R}^{n_u}.$$

To prove (C3), it now suffices to notice that for each  $t \in [0, T_S]$ , one has

$$\|x(0)\|^2 - \|x(t)\|^2 \leq 2 \left| \int_0^t x^\top(\tau) \dot{x}(\tau) d\tau \right| \leq 2\mathcal{C} \int_0^{T_S} (\|x(\tau)\|^2 + \|u(\tau)\|^2) d\tau = 2\mathcal{C}\Psi(x, u).$$

Integrating over  $t \in [0, T_S]$ , one proves thus that

$$T_S \|x(0)\|^2 - \Psi(x, u) \leq \int_0^{T_S} (\|x(0)\|^2 - \|x(t)\|^2) dt \leq 2\mathcal{C}T_S\Psi(x, u),$$

entailing thus (C3) with  $M = 2\mathcal{C} + T_S^{-1}$ .  $\square$

Notice that  $T_S$  in Proposition C.7 can be replaced by an arbitrary  $T > 0$  (the constant  $M$ , of course, will depends on  $T$  in this case). The following corollary is now immediate, illustrating that  $V_{\mathbf{P}}$  is positive definite uniformly in  $\mathbf{P}$  (which matrix has to be large enough to keep the solutions uniformly bounded).

**Corollary C.8.** *A constant  $\alpha > 0$  exists such that for all  $x_0 \in \mathcal{R}_0(T_p)$  and  $\mathbf{P} = \mathbf{P}^\top > p_0 I$*

$$V_{\mathbf{P}}(x_0) \geq \Psi(\hat{x}_{[0, T_S]}, \hat{u}_{[0, T_S]}) \geq \alpha \|\hat{x}(t)\|^2 \quad \forall t \in [0, T_S]. \quad (\text{C4})$$

Here  $p_0$  is the constant from Theorem 5.7 and  $(\hat{x}, \hat{u})$  is the minimizer in  $\mathbf{OCP}(0, x_0)$ .

**Proof.** The left inequality in (C4) is trivial, so it suffices to prove the rightmost one.

As has been already proved (Theorem 5.7), the optimal solution in (C1) stays in  $\mathcal{D} = \mathcal{R}_0(T_p + T_S)$ . Choosing  $\beta = M^{-1}$ , one has

$$\psi \doteq \Psi(\hat{x}_{[0, T_S]}, \hat{u}_{[0, T_S]}) \geq M^{-1} \|x_0\|^2,$$

where  $M$  is the constant from Proposition C.7 corresponding to  $\mathcal{D}$ . Retracing the proof of Proposition C.7 (where  $x, u$  have to be replaced by  $\hat{x}, \hat{u}$ ), one demonstrates that

$$\|\hat{x}(t)\|^2 - \|x_0\|^2 \leq 2\mathcal{C}\psi \quad \forall t \in [0, T_S],$$

where  $\mathcal{C}$  is some constant (by the set  $\mathcal{D}$ ), and hence the rightmost inequality in (C4) holds for  $\alpha \doteq (M + 2\mathcal{C})^{-1}$ .  $\square$

*A Lyapunov-like property for the sampled states  $x(t_k)$*

Proving Theorem 5.7, a substantially stronger statement has been established: by choosing  $\mathbf{P}$  large enough, we can guarantee that the optimal solution to  $\mathbf{OCP}((0, x_0))$  arrives at the point  $\bar{x} \doteq \hat{x}(T_p)$  with an arbitrarily small predesigned norm, and thus provide that  $\hat{x}(T_p) \in \mathcal{R}_0(T)$  with an arbitrary small  $T < T_S$ . Figure C1 inspires the following admissible (possibly, non-optimal) control  $\hat{u}^+$  in the problem  $\mathbf{OCP}(T_S, \hat{x}(T_S))$

$$\hat{u}^+(t) = \begin{cases} \hat{u}(t), & t \in [T_S, T_p], \\ u_{T, \bar{x}}(t - T_p), & t \in [T_p, T_p + T], \\ 0, & t \in [T_p + T, T_p + T_S]. \end{cases}$$

Here  $\hat{u}$  is the optimal control in  $\mathbf{OCP}((0, x_0))$  and  $u_{T, \bar{x}} : [0, T] \rightarrow U_C$ , as previous, is the control driving the state vector from  $x(0) = \bar{x}$  to  $x(T) = 0$ . The corresponding state trajectory  $\hat{x}^+ : [T_S, T_S + T_p] \rightarrow \mathbb{R}^{n_x}$ , obviously, coincides with  $\hat{x}(t)$  on  $[T_S, T_p]$ , equals  $x_{T, \bar{x}}(t - T_p)$  when  $t \in [T_p, T_p + T]$  and is zero when  $t \in [T_p + T, T_p + T_S]$ , nullifying thus the terminal cost. Using the rightmost inequality in (C2), one has

$$\begin{aligned} V_{\mathbf{P}}(\hat{x}(T_S)) &\leq J_{\mathbf{P}}(\hat{x}^+, \hat{u}^+) = \int_{T_S}^{T_p} \Phi(\hat{x}(\tau), \hat{u}(\tau)) d\tau + \tilde{c}(T) = \\ &= V_{\mathbf{P}}(x_0) + \tilde{c}(T) - \int_0^{T_S} \Phi(\hat{x}(\tau), \hat{u}(\tau)) d\tau \leq V_{\mathbf{P}}(x_0) + \tilde{c}(T) - \alpha \|x_0\|^2. \end{aligned} \quad (\text{C5})$$

(the last inequality is implied by the rightmost inequality in (C4)). Recalling that  $\tilde{c}(T)$  can be done arbitrarily small by providing that  $\|\hat{x}(T_p)\|$  belongs to a ball of a sufficiently small radius, which, in turn (see the proof of Theorem 5.7) can be guaranteed by choosing the weight matrix  $\mathbf{P}$  large enough, one arrives at the following important lemma.

**Lemma C.9.** *Let  $x_0 \in \mathcal{R}_0(T_p)$ . Then, for any  $\eta > 0$  there exists  $\bar{p} = \bar{p}(\eta)$  such that if  $\mathbf{P} \geq \bar{p}I$ , then the optimal state trajectory in  $\mathbf{OCP}(0, x_0)$  satisfies the inequality*

$$V_{\mathbf{P}}(\hat{x}(T_S)) - V_{\mathbf{P}}(x_0) \leq \eta - \alpha \|x_0\|^2,$$

where  $\alpha$  is the constant from (C4).

Generalizing this lemma to the  $\mathbf{OCP}(t_k, x(t_k))$  solved by our NMPC, the following corollary is immediate.

**Corollary C.10.** *For each  $\eta > 0$  there exists  $\bar{p} = \bar{p}(\eta)$  such that if  $\mathbf{P} \geq \bar{p}I$ , then  $V_{\mathbf{P}}$  is featured by the following Lyapunov-type property on the time-sampled state trajectory:*

$$V_{\mathbf{P}}(x(t_{k+1})) - V_{\mathbf{P}}(x(t_k)) \leq \eta - \alpha \|x(t_k)\|^2, \quad (\text{C6})$$

provided that the initial condition  $x(0)$  (and hence, all  $x(t_k)$ ) belongs to  $\mathcal{R}_0(T_p)$ .

#### C.4. Proof of Theorem 5.8

We are now ready to prove Theorem 5.8. The proof is divided into several steps.

**Step 1.** For a given constant  $\eta > 0$ , we fix the weight matrix  $\mathbf{P} \geq \bar{p}(\eta)I$ , which, according to Corollary C.10, entails (C6) for any solution starting at  $x(0) \in \mathcal{R}_0(T_p)$ . Denote

$$r(\eta) \doteq (2\eta/\alpha)^{1/2}, \quad v(\eta) \doteq \sup_{x \in \mathbf{B}_{r(\eta)} \cap \mathcal{R}_0(T_p)} V_{\mathbf{P}}(x) < \infty$$

(notice that the supremum is finite thanks to Corollary C.5).

Consider the solution of the closed-loop system, starting at  $x(0) \in \mathcal{R}_0(T_p)$ . Then we know that  $x(t_k) \in \mathcal{R}_0(T_p)$  for all  $k$  (Theorem 5.7). We claim that an index  $m \geq 0$  exists such that  $x(t_m) \in \mathbf{B}_{r(\eta)}$ . Indeed, if  $x(t_k) \notin \mathbf{B}_{r(\eta)}$ , then, according to C.10, one has

$$V_{\mathbf{P}}(x(t_{k+1})) - V_{\mathbf{P}}(x(t_k)) \leq -\eta < 0,$$

which inequality, in view of nonnegativity of  $V_{\mathbf{P}}$ , cannot hold for all  $k \geq 0$ .

**Step 2.** We claim that for all  $k \geq m$ , the inequality holds as follows

$$V_{\mathbf{P}}(x(t_k)) \leq v(\eta) + \eta. \quad (\text{C7})$$

To prove this, we use induction on  $k$ . For  $k = m$ , we obviously have  $V_{\mathbf{P}}(x(t_k)) = V_{\mathbf{P}}(x(t_m)) \leq v(\eta)$ , because  $x(t_m) \in \mathbf{B}_{r(\eta)} \cap \mathcal{R}_0(T_p)$ . Assuming that (C7) holds for  $k$ , we can easily prove it for  $k + 1$  by considering two cases:

- if  $x(t_k) \in \mathbf{B}_{r(\eta)}$ , then  $V_{\mathbf{P}}(x(t_k)) \leq v(\eta)$  and, using (C6), it is obvious that

$$V_{\mathbf{P}}(x(t_{k+1})) \leq V_{\mathbf{P}}(x(t_k)) + \eta \leq v(\eta) + \eta.$$

- if  $x(t_k) \notin \mathbf{B}_{r(\eta)}$ , then (C6) entails that  $V_{\mathbf{P}}(x(t_{k+1})) < V_{\mathbf{P}}(x(t_k)) \leq v(\eta) + \eta$ , where the last inequality is implied by the induction hypothesis.

**Step 3.** Using Corollary C.8 (where  $x_0 = x(t_k)$ ,  $k \geq m$  and  $\hat{x}(t) = x(t_k + t)$  for all  $t \in [0, T_S]$ ), one guarantees that

$$\|x(t)\|^2 \leq \alpha^{-1}(\eta \leq v(\eta) + \eta) \quad \forall t \geq t_m$$

provided that  $\mathbf{P} \geq \bar{p}(\eta)I$ .

To finish the proof of Theorem 5.8, it suffices to notice that  $v(\eta) \rightarrow 0$  as  $\eta \rightarrow 0$  thanks to Corollary C.6. Hence, choosing  $\eta = \eta(\varepsilon_*) > 0$  small enough, it is possible to guarantee (32) for each predefined  $\varepsilon_* > 0$ , provided that  $\mathbf{P} \geq p_*I$ , where  $p_* = r(\bar{\eta}(\varepsilon_*))$ .